AEROSPACE APPLICATIONS OF SINDA/FLUINT AT THE JOHNSON SPACE CENTER

Michael K. Ewert
NASA Johnson Space Center
Houston, Texas

Phillip E. Bellmore
McDonnell Douglas Space Systems Co.
Houston, Texas

Kambiz K. Andish, John R. Keller
Lockheed Engineering & Sciences Co.
Houston, Texas

ABSTRACT

SINDA/FLUINT has been found to be a versatile code for modeling aerospace systems involving single or two-phase fluid flow and all modes of heat transfer. The code has been used successfully at the Johnson Space Center (JSC) for modeling various thermal and fluid systems. Features of the code which have been utilized include transient simulation, boiling and condensation, two-phase flow pressure drop, slip flow, multiple submodels and depressurization. SINDA/FLUINT has been used at JSC to support the Space Shuttle, Space Station Freedom and advanced programs. Several of these applications of SINDA/FLUINT at JSC are described in this paper.

SINDA/FLUINT is being used extensively to model the single phase water loops and the two-phase ammonia loops of the Space Station Freedom active thermal control system (ATCS). These models range from large integrated system models with multiple submodels to very detailed subsystem models. An integrated Space Station ATCS model has been created with ten submodels representing five water loops, three ammonia loops, a Freon loop and a thermal submodel representing the air loop. The model, which has approximately 800 FLUINT lumps and 300 thermal nodes, is used to determine the interaction between the multiple fluid loops which comprise the Space Station ATCS.

JSC has also developed several detailed models of the flow-through radiator subsystem of the Space Station ATCS. One model, which has approximately 70 FLUINT lumps and 340 thermal nodes, provides a representation of the ATCS low temperature radiator array with two fluid loops connected only by conduction through the radiator face sheet. The detailed models are used to determine parameters such as radiator fluid return temperature, fin efficiency, flow distribution and total heat rejection for the baseline design as well as proposed alternate designs.

SINDA/FLUINT has also been used at JSC as a design tool for several systems using pressurized gasses. One model examined the pressurization and depressurization of the Space Station airlock under a variety of operating conditions including convection with the side walls and internal cooling. Another model predicted the performance of a new generation of manned maneuvering units. This model included high pressure gas depressurization, internal heat transfer and supersonic thruster equations. The results of both models were used to size components, such as the heaters and gas bottles and also to point to areas where hardware testing was needed.

INTRODUCTION

Use of the Systems Integrated Numerical Differencing Analyzer (SINDA) analysis tool has expanded steadily over the years since its origin in the 1960's. The Fluid Integrator (FLUINT) code added significant fluid system analysis capabilities under a NASA Johnson Space Center (JSC) contract in 1985 (ref. 1). Since then, analysis applications for the code have increased in scope as well as in number. At the Johnson Space Center, SINDA/FLUINT has been used to solve both steady state and transient thermal/ hydraulic problems involving single and two-phase fluid flow with heat transfer. Conduction, convection and radiation have been modeled in simple and complex systems alike. Models have ranged from a few nodes to a few thousand nodes. SINDA/FLUINT has been used at JSC to support the Space Shuttle, Space Station Freedom (SSF) and other advanced technology programs. The code has been used in the conceptual design, detailed design, test and performance verification phases of these programs.

The Space Station Thermal Control System (TCS) consists of both passive thermal control features and active fluid loops to transport heat. The power system uses a single-phase ammonia cooling system and the habitable modules use single-phase water loops to gather heat from racks filled with equipment. The internal thermal control system (ITCS) water loops transfer their heat to one of three external thermal control system (ETCS) two-phase ammonia loops which dump the heat to space. Figure 1 shows a schematic representation of the Permanently Manned Capability (PMC) Space Station Freedom and indicates the location of some of the TCS features. Thousands of SINDA/FLUINT CPU hours have been logged analyzing the various Space Station Freedom Thermal Control Systems during the design phase, and this use will continue into the operational phase since SINDA/FLUINT is the official code used for Space Station Integrated Thermal Analysis. SINDA/FLUINT submodels developed by various system designers are integrated and run at JSC in order to analyze integrated system performance under various nominal and off-nominal conditions.

Other more detailed SINDA/FLUINT models have been built of particular components of the SSF Active Thermal Control System (ATCS), particularly the ETCS radiators. These radiators have undergone several redesigns in order to improve performance and reduce weight, cost and assembly time. SINDA/FLUINT has been used in these design trade studies in order to evaluate potential alternate designs. One such study, which will be described here, looked at ways to prevent the radiators from freezing when subjected to an environment temperature substantially below the freezing point of the ammonia working fluid.

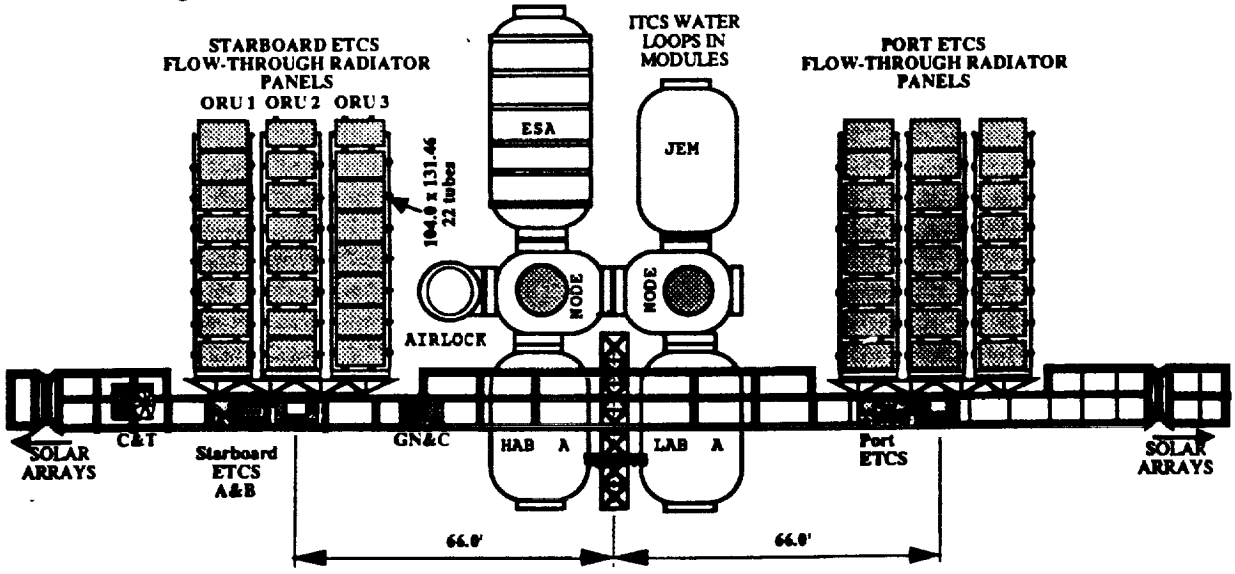

Figure 1: PMC Configuration of Space Station Freedom

Ideal gas systems are another area in which SINDA/FLUINT has been used successfully. Using the "volume flowrate set" (VFRSET) feature in SINDA/FLUINT to model a vacuum pump, the Space Station airlock has been modeled during depressurization and hyperbaric operations. Other features of the code have been used to model the storage tank and thrusters of a new manned maneuvering unit.

SPACE STATION FREEDOM INTEGRATED THERMAL ANALYSIS

SINDA/FLUINT has been utilized in support of Space Station Freedom Integrated Active Thermal Analysis. This task is responsible for integrating SINDA/FLUINT math models of all space station active thermal control systems and analyzing the resultant math model under a variety of conditions. Analyzed conditions include nominal and off-nominal operations.

Analysis of nominal operations generally consists of utilizing a time variant applied heat load and environmental conditions and determining if the system response is acceptable. Off-nominal analysis would consist of such conditions as pump failures, control system failures, imbalances between applied and rejectable heat loads, and system startups/shutdowns. The SINDA/FLUINT models have been used to analyze all of the above transients. The SINDA/FLUINT models will be briefly described and examples of problems solved will be given.

SINDA/FLUINT Model Descriptions

The SINDA/FLUINT models utilized consist of two basic types - the models of the internal habitable modules (internal thermal control system - ITCS) and the models of the external two-phase ammonia heat transport system (external thermal control system - ETCS). The models of the internal systems consist of the United States resource nodes, the United States habitation and laboratory modules, the Japanese experiment module, and the European Space Agency Columbus module. For all modules, both a detailed and a simplified version of the models have been developed.

The modeling philosophy utilized for the detailed ITCSs is to provide sufficient resolution so that the exit temperature of each experiment rack or equipment rack can be determined and the majority of conceivable configurations and transients can be accurately modeled. The transient response time is also considered in order to accurately predict the energy transport to the ETCS. The models do not consider the temperatures of the individual coldplates within a rack, of which there can be from 4 to 8 in each rack. The nodalization for detailed models typically consists of 150 to 200 FLUINT nodes. These models are used to evaluate system cooling, controls stability, pump sizing, and off-nominal performance.

For the simplified ITCS models, the response desired is the overall module response to total module heat load changes. The simplified models are typically used to provide more realistic boundary conditions for the ETCS. Therefore, the nodalization can typically consist of fewer than 20 FLUINT nodes.

United States Habitation and Laboratory System and Model Description

The U.S. habitation (U.S. Hab) module is the primary living quarters for the Space Station occupants, while the laboratory (U.S. Lab) module is the primary U.S. location for research. Both modules utilize an ITCS architecture that nominally acts as a two-loop system but is capable of being reconfigured as a one-loop system (Figure 2). When in two-loop mode, the section connected to the low temperature interface heat exchanger (IHX) is termed the LT branch and the section connect to the moderate temperature IHX is termed the MT branch. The two-loop to one-loop architecture is prevalent onboard the Space Station, being utilized by all U.S. modules and currently being considered by the International Partners.

The U.S. Hab/Lab system uses a System Flow Control Assembly to maintain a constant pressure drop between the rack supply and the rack return lines. The maintenance of the constant "delta-p" helps ensure adequate flow to each rack. The flow to a particular rack is controlled by the Rack Flow Control Assemblies which monitor either temperature or flowrate, depending on the particular type of control desired. Variation of a rack's flowrate is necessary to conserve power since not all racks will require cooling at all times. The U.S. Hab/Lab system also includes a regenerative heat exchanger that is used to ensure that the water entering the MT branch is above 60°F (15.5°C). The 60°F setpoint was chosen since the Space Station maximum allowable dewpoint is 60°F, thus precluding condensation on the MT branch of plumbing and saving the expense of insulating the entire system. Each Interface Heat Exchanger (IHX) has a bypass line that is used to maintain a desired overall IHX outlet temperature.

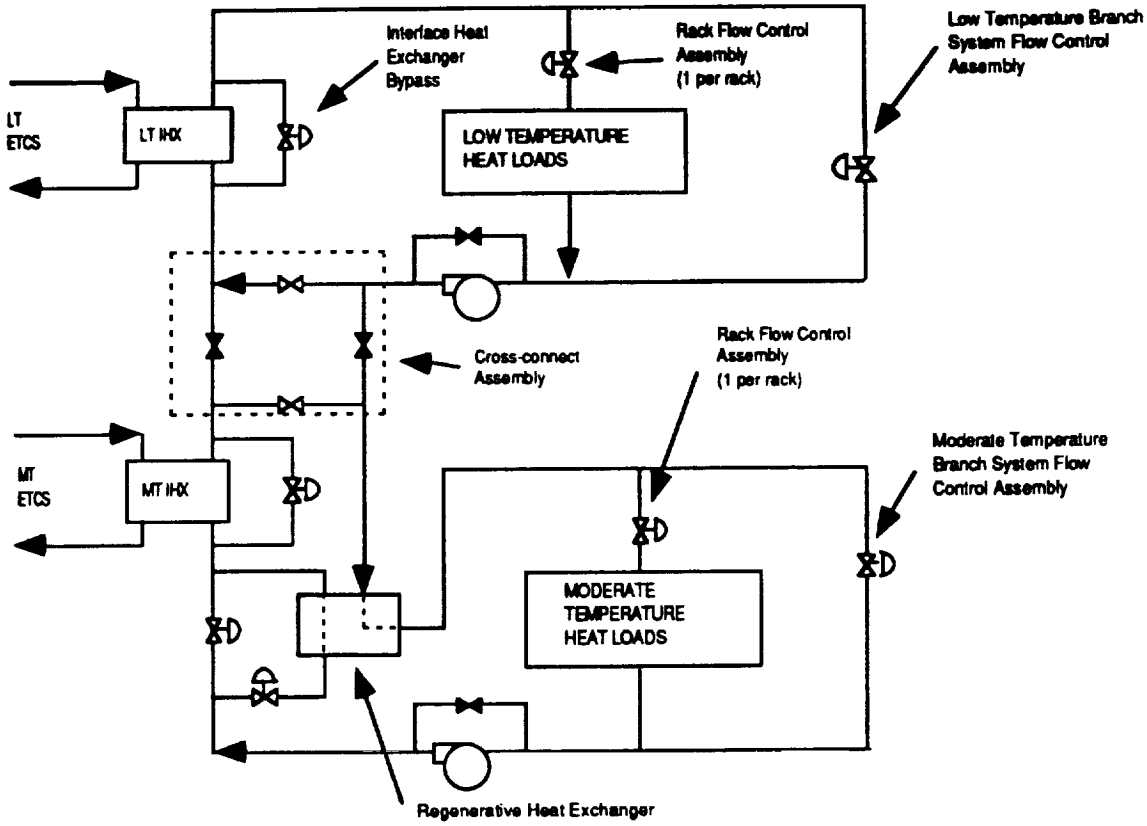

Figure 2. United States Habitation/Laboratory Functional Schematic

The FLUINT models of the habitation and laboratory modules are similar, the primary difference being the number of payload and system racks. The level of detail is such that all racks are modeled as well as important control systems. Figure 3 provides a schematic showing the number and location of the FLUINT components for the U.S. Laboratory module.

For the U.S. Lab model, most fluid line lengths and sizes have been defined and have been incorporated. The locations of elbows and some connections have not yet been defined. The control valve characteristics, such as k-loss and flow areas, have been defined for the Rack/System Flow Control valves. The characteristics for the remainder of the valves are not yet defined. The Rack/System Flow Control valve is a sculpted ball valve with a variable k-loss. This action is modeled within FLUINT by altering both the valve angle and the k-loss value. The thermal mass of the equipment in each rack is accounted for by including a SINDA thermal node equivalent to 30 lb_m (13.62 kg) of stainless steel, though the actual mass of equipment in each rack is currently unknown.

The fluid pump head curve has been defined and is incorporated into the FLUINT model. The FLUINT pump model is strictly valid only in the first quadrant of operation, i.e. windmilling, reverse flow, etc., can not be predicted. The model can predict changes in pump operation due to changes in speed.

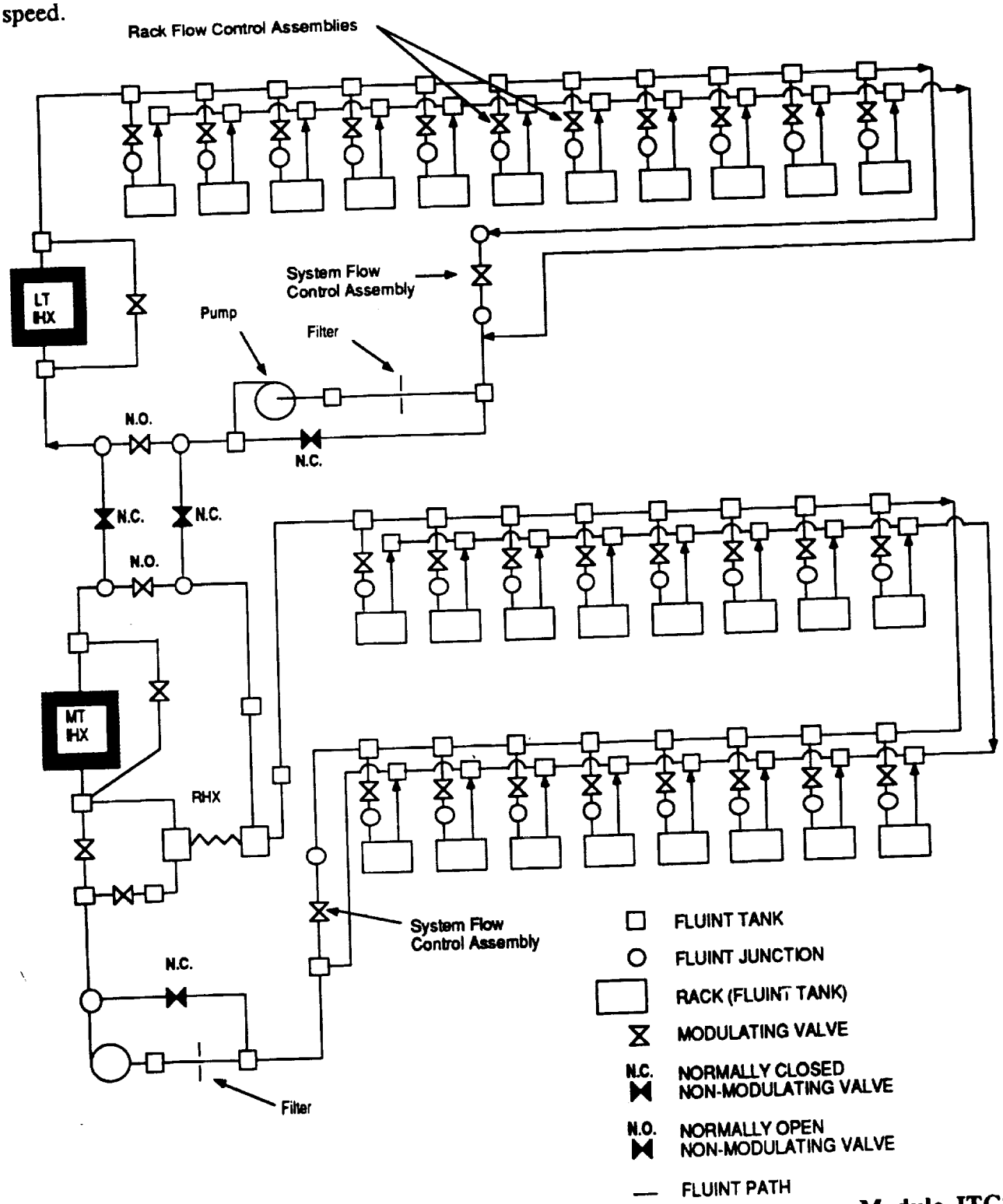

Figure 3. FLUINT Nodalization of the United States Laboratory Module ITCS

The model of the U.S. Hab maintains the same level of detail, though the number of FLUINT components is reduced since the U.S. Hab has fewer racks.

Resource Node System and Model Description

The resource node contains the primary command and control avionics for the Space Station. The resource node ITCS cools the resource node 2, resource node 1, airlock and Pressurized Logistics Module (PLM). The PLM can be located at either resource node 1 or resource node 2. Since the airlock, resource node 1 and PLM are attached at different stages of the Space Station construction, and possibly at different locations for the PLM, several distinct configurations of the resource node ITCS exist. This variability forces special modeling considerations for the resource node and will discussed below. The architecture of the resource node is the most developed at this time since the resource node will be the first habitable module launched. Therefore, the FLUINT model of the resource node is the most complex and also the most useful for predicting ITCS performance.

The ITCS for the resource node is a simplified variant of the ITCS for the U.S. laboratory module discussed above. Unlike the U.S. Hab/Lab systems, the equipment in the resource node is normally always on. Therefore, the need to provide a variable flowrate is not present. The ITCS developers have chosen to use an orifice to control the flow to each rack with the coolant pumps set to a constant speed. There are some active components associated with the resource node, the primary ones being rack flow control valves associated with the PLM. These valves will modulate to maintain a constant exit temperature for each PLM rack. Also associated with the PLM is a modulating delta-pressure valve which acts to maintain a constant pressure for the inlet header to the PLM racks.

The detailed FLUINT model of the resource node uses the same component descriptions and modeling as the U.S. Hab/Lab due to common hardware. Such items as IHX bypass valves, RHX modeling, and pump modeling are identical. The modeling of the rack is also the same. Modeling specific to the resource node involves the level of detail of the plumbing and the variability in the configuration.

The geometry of the resource node is established sufficiently such that three-dimensional isometric drawings, with dimensions, have been generated. These drawings allow for a more accurate definition of ITCS line length. Also, the pressure drop effect of elbows and bends can be estimated using the effective length approach. Though the FLUINT model does not yet consider the effect of fluid connectors, such as tees and quick disconnects, the actual connectivity of the ITCS can now be included into the model, with the pressure drop data included when available.

The variability of the resource node configuration results in four unique configurations, not counting the position of the PLM. The multiple configurations of the ITCS are accounted for by utilizing the capability of FLUINT to include sections of input from predefined external files. Each module is contained in a separate input file and included as necessary to create the ITCS connectivity of the particular configuration. The use of external files allows for easy maintenance of the various portions of the resource node ITCS model. Should a particular module change, only the model of that module need be altered to make the change effective for all configurations. The alternative would be to make changes to as many as eight separate models, which could lead to errors in implementation.

International Partners System and Model Description

The International Partners, the European Space Agency (ESA) and the National Space Development Agency of Japan (NASDA), are currently in the process of re-designing their respective ITCSs. The baseline design for both is a one-loop system with temperature controlling bypasses. The re-design efforts are due to problems in meeting Space Station thermal load management goals. The final configuration will not be known for several months, however some of the basic components will probably still exist.

The ESA ITCS is similar in concept to the resource node ITCS. The coolant flow to each primary payload rack is controlled via an orifice. In parallel with the racks is an avionics heat exchanger. The

outlet temperature of the avionics heat exchanger is controlled to a setpoint by a modulating valve. The operation of the valve will cause pressure variations at the inlet of the heat exchanger and also the payload racks. The coolant pump's speed is controlled to maintain a constant pressure at the inlet of the racks.

The NASDA ITCS contains several dedicated cooling loops which interface with the main cooling loop via heat exchangers. Of particular interest is a Freon cooling loop which services an external platform. The ability to model multiple fluids, while not unique to FLUINT, enhances the range of problems that FLUINT can be applied to. The NASDA ITCS has a combination of orificed and actively controlled payload rack locations. Pump speed is controlled based both on pressure and temperature inputs.

Models of several proposed International Partners ITCSs have been created and utilized to perform analysis. The analysis has concentrated on verifying the general acceptability of proposed design changes and will be discussed in more detail below. SINDA/FLUINT has shown to be a very versatile and well-behaved analysis tool during the course of these numerous modifications.

External Thermal Control System and Model Description

The External Thermal Control System (ETCS) is the primary method for transporting the waste heat generated within the habitable modules for ultimate rejection to space. The ETCS is a two-phase ammonia system with several unique components such as the Rotary Fluid Management Device (RFMD), Back Pressure Regulating Valve (BPRV), and cavitating venturies. Additional components include two-phase ammonia to single-phase water heat exchangers, condensing radiators, a bellows accumulator, two-phase coldplates, and associated plumbing. The ETCS has three separate cooling loops, two Low Temperature (LT) loops operating from 33 to 39°F (1 to 4°C) and one Moderate Temperature (MT) loop operating from 55 to 62°F (13 to 17°C). Figure 4 provides an ETCS functional schematic for the Man Tended Configuration of SSF.

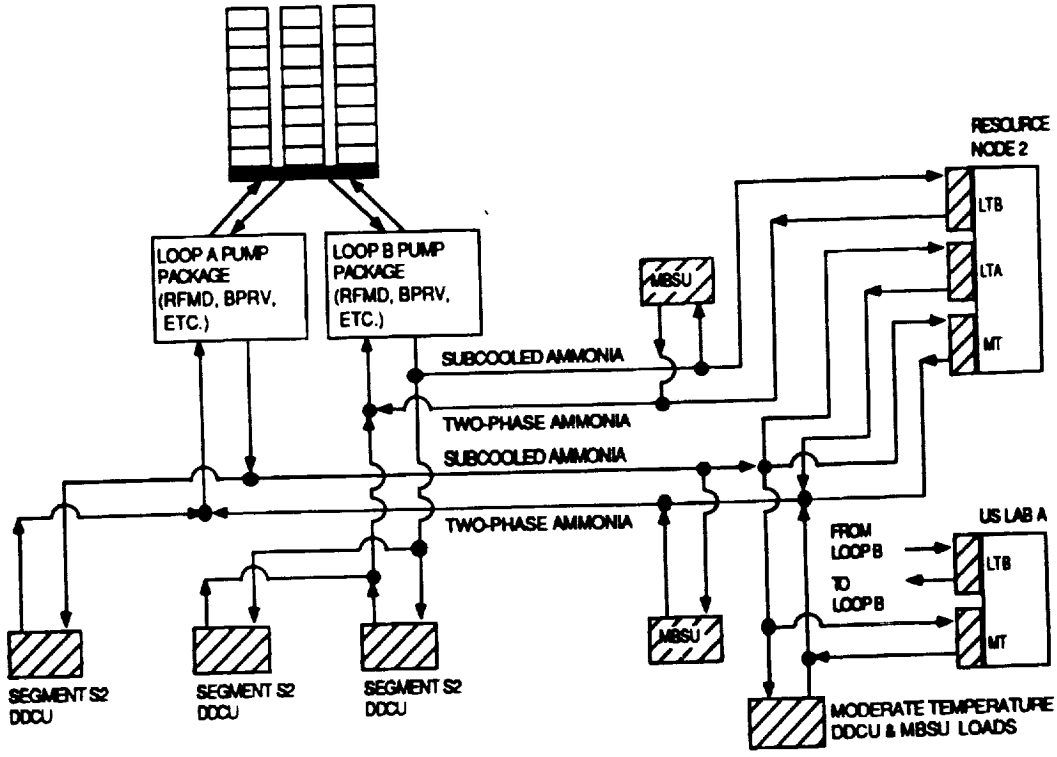

Figure 4. ETCS Functional Schematic for the Man Tended Configuration

The system operation consists of the RFMD suppling slightly subcooled ammonia liquid to a distributed system of heat exchangers. The flow to each heat exchanger, and therefore the ultimate heat acquisition capability of each heat exchanger, is controlled by a cavitating venturi placed at the inlet of each heat exchanger. The downstream pressure is controlled so that the ammonia will be very close to the saturation point after exiting the cavitating venturi. With the addition of heat from the internal modules, the ammonia begins to boil, enhancing the heat transfer process. The heat transferred to the ammonia is controlled so that the maximum ammonia vapor quality is no greater than 90%. The resulting two-phase mixture returns to the RFMD.

The RFMD consists of a stationary outer housing with a rotating inner housing that acts to separate the two-phase mixture into vapor and liquid components (Figure 5). The ammonia vapor is plumbed to the condensing radiators where the acquired heat is rejected to space. The condensate then returns to the RFMD where its temperature is increased and then pumped back out to the module's heat exchangers. The pumping action of the RFMD is via immersed pitot probes which convert the rotational energy into a static pressure rise, thus providing the necessary pumping power. The RFMD maintains an internal liquid level by means of a level pitot which acts to pump excess fluid to the bellows accumulator.

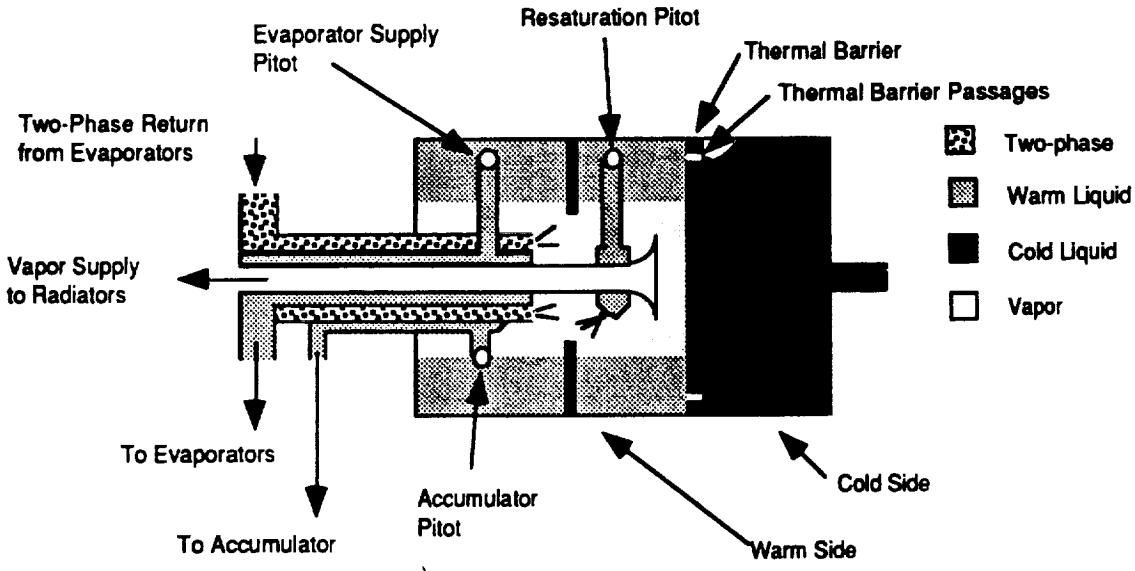

Figure 5. Rotary Fluid Management Device Schematic

Since the ETCS is a two-phase system, the operating pressure controls the operating temperature. The Back Pressure Regulating Valve is designed to passively control the pressure in the RFMD. The BPRV does this through a combination of spring and servo action (Figure 6). The system is also capable of changing operating temperatures by altering the relative spring forces inside the BPRV, thus temporarily affecting the heat rejection rate and raising or lowering the system pressure.

The modeling of the ETCS can be broken down into two distinct portions; the first being the modeling of the pump module assembly (RFMD, BPRV, and bellows accumulator) and radiator and the second being the remainder of the system (main plumbing, cavitating venturies, and module heat exchangers). The model of the pump module assembly consists of a detailed description of the RFMD, BPRV, and bellows accumulator. The model considers the physics of the RFMD by determining parameters such as the induced gravity head due to the rotation, pumping power from the pitot probes, and internal liquid levels. The model of the BPRV uses the internal geometry, including spring forces and internal bellows areas, to calculate the forces on the primary pressure control valve. The condensing radiator model is of moderate detail and accounts for thermal interactions between the parallel flow passages.

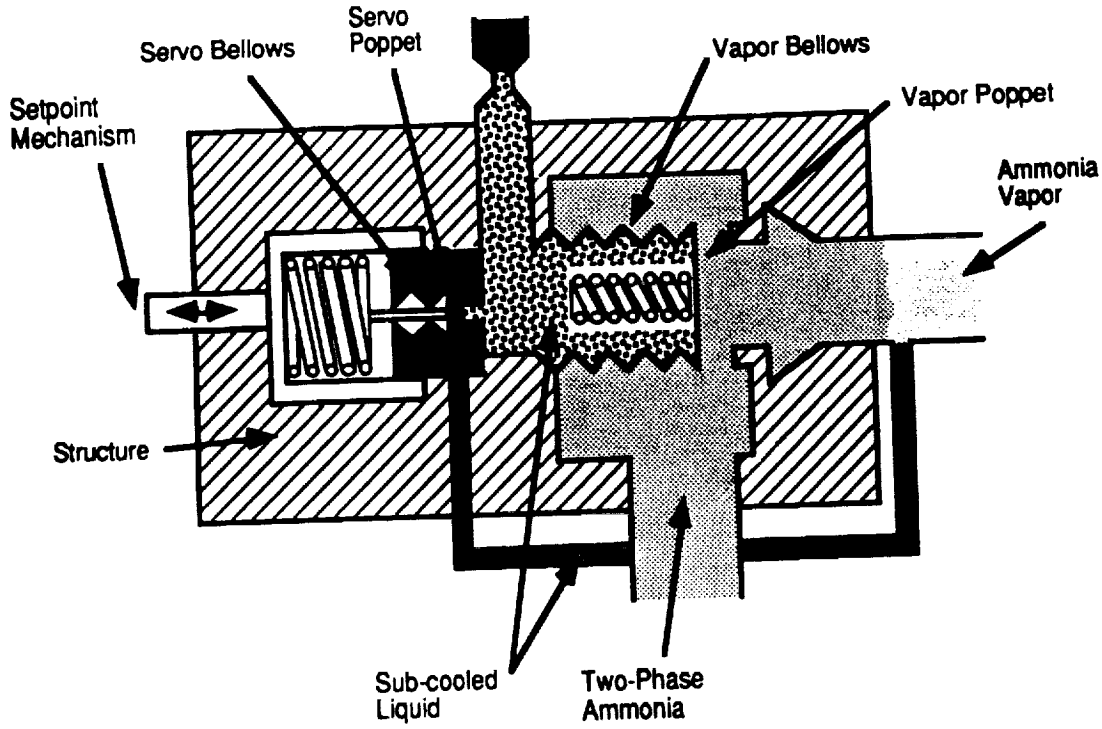

Figure 6. Back Pressure Regulating Valve Schematic

The model of the remainder of the system includes geometrically correct representations of the ETCS plumbing lengths, internal diameters, and plumbing routing. The correct geometry is critical to allow for accurate predictions of system pressure drops. The model takes advantage of the recently included option in FLUINT to determine pressure drops based on the flow regime.

Models of the cavitating venturies and module heat exchangers are also included. Due to the geometrically difficult phenomenon of the cavitating venturies, they are modeled utilizing a vendor supplied equation applicable for nominal conditions. Determination of cavitating venturi response during off-nominal conditions is still being investigated. The module heat exchangers are modeled as a single heat acquisition point since no details regarding the heat exchanger geometry are currently available. Figure 7 provides the FLUINT nodalization of the Moderate Temperature Loop for the Permanent Manned Capability configuration. The Low Temperature Loop's nodalization is similar.

Summary of Analyses Performed with the SSF Integrated ATCS Models

The models described above are used to analyze the Space Station active thermal control systems in both stand-alone and integrated modes. In stand-alone mode, the models are usually used to investigate control system dependencies, system pressure drops, and internal effects due to specific external conditions. These models have assisted in the detection and quantification of several system performance issues for both the United States and the International Partners.

For the United States modules, the models identified a mal-distribution of module waste heat onto the ETCS which could have caused an overload of the ETCS. Following a re-design of the U.S. modules, the FLUINT models assisted in control system development for the Resource Node. Also, the models were used to identify a potential water vapor condensation problem on a portion of the plumbing

that was un-insulated. The models were used to evaluate various options and to quantify the heat load value at which condensation became a potential problem.

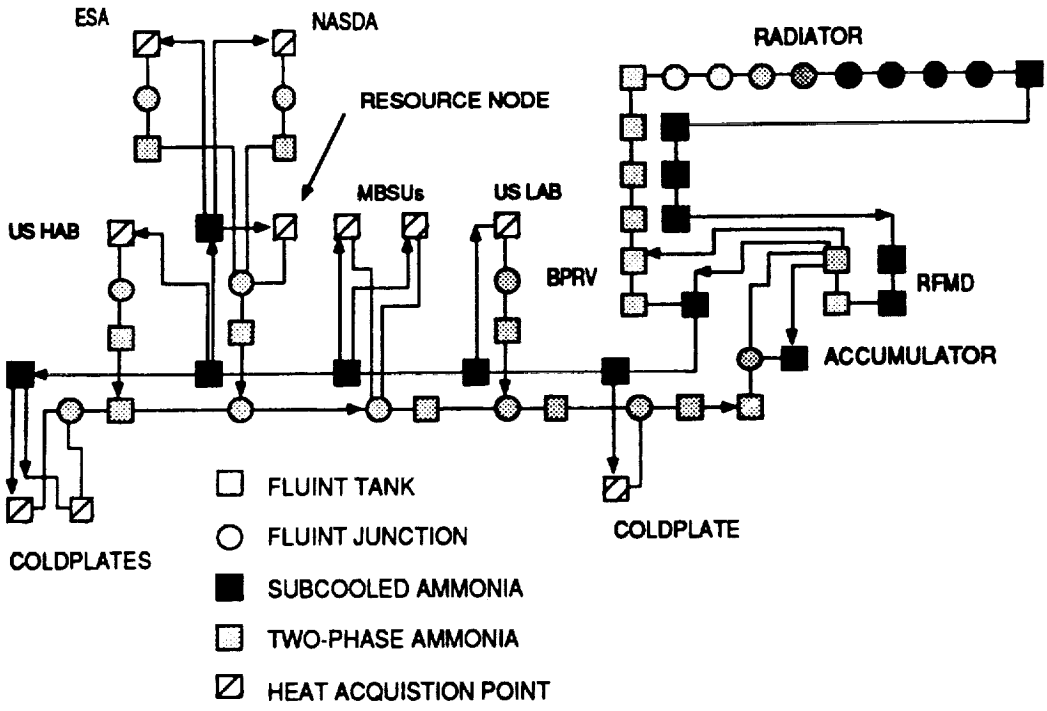

Figure 7. FLUINT Nodalization of the Moderate Temperature Loop for PMC

For the International Partners, the models identified a similar mal-distribution of module waste heat that violated Space Station operating specification. Several IP proposed options were modeled and evaluated as to the option's ability to meet station requirements. Additionally, the models have been used to evaluate control system stability.

In the integrated mode, the models have identified several key system issues and been used to analyze system operation at off-nominal conditions. One system issue identified was the inadequate heat load placed on one of the loops of the ETCS during early operations. The ETCS nominally consists of three loops - two Low Temperature and one Moderate Temperature. The Low Temperature loops are the first activated during the early stages of space station construction, when the total heat loads are the lowest. The pump module assembly requires a minimum amount of heat load (about 1.5 kW) to ensure adequate operation of the BPRV. Integrated analysis showed that only about 1 kW of thermal load was present on one of the Low Temperature loops during certain portions of station construction. The integrated models were used to devise methods to shift heat load from one Low Temperature loop to the other by altering the operating temperatures. Also identified by analysis in the integrated mode was the possibility of ammonia freezing in the condensing radiators due to low heat loads and cold external environments. The radiator manufacturer has confirmed this possibility and the design is being modified to account for freezing.

Off-nominal analysis has involved investigating the impacts to the system when operated at elevated temperatures. Operation at elevated temperatures enhances the heat rejection capability but can adversely impact the atmospheric temperatures inside the habitable modules. Since this change impacted the habitable modules, a coordinated analysis effort with the module providers was necessary. The ease with which the SINDA/FLUINT models can be changed allowed for rapid evaluation of proposed operating points.

The integrated models are currently being used to investigate the initial activation of the resource node, which is the first habitable module attached to the Space Station, and the impact of ETCS flow variations on both the ETCS and the internal modules. Other system responses being investigated are the transient response to operating temperature changes and the impact of large heat load changes, such as would occur during the re-activation of a module that was temporarily shut down.

DETAILED RADIATOR MODELS

Radiator Panel Description

Heat rejection in the Space Station ETCS occurs by condensation of ammonia in small diameter tubes of thermal radiators that radiate the heat to deep space. The radiators are designed to reject a total of 82.5 kW of waste heat. Of this, 49.0 kW is allocated to the moderate temperature (MT) loop and the remaining 33.5 kW is allocated to the two low temperature (LT) loops. The radiators are sized to satisfy heat rejection requirements of the LT radiators at a worst case design environment. This leads to a total heat rejection area of 4557 ft^2 (423.3 m^2) for the LT loop radiators. The permanently manned capability (PMC) configuration of SSF has a total of 48 radiator panels grouped in 3 orbital replacement units (ORUs) of 8 panels, on each side of the Space Station, as shown in Figure 1. Each radiator panel consists of 22 thin-wall flow tubes manufactured of stainless-steel for ammonia compatibility. Each tube is 120.9" (3.070 m) long and has an inner diameter of 0.067" (1.7 mm). The flow tubes are inserted in a tube extrusion made of 6061-T6 aluminum alloy for high conductivity and low weight. Each tube extrusion is 0.67" (17.0 mm) tall with flat interfaces 0.232" (5.9 mm) wide on top and bottom. A very thin layer of thermal adhesive (0.003", 0.076 mm) is used between the stainless-steel flow tube and the aluminum extrusion to assure a good thermal contact between the two surfaces. The tube extrusions are bonded between two 6061-T6 aluminum face sheets 120.9" x 104.0" (307 cm x 264 cm) and 0.01" (0.254 mm) thick. The exposed surfaces of the face sheets are coated with a 0.005" (0.127 mm) thick film of Z93 paint for better radiative properties. Details of the flow tube and the extrusion are shown in Figure 8.

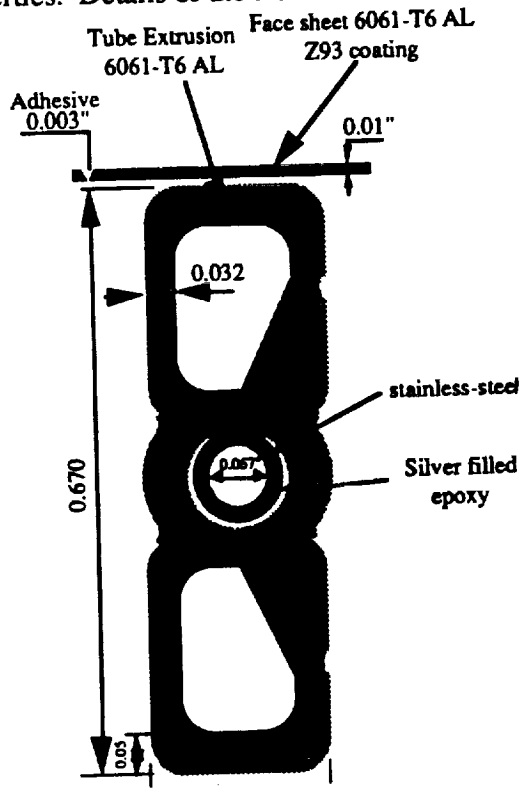

Figure 8 : Detail of the Tube Extrusion

Two separate sets of manifold tubes (manifolds A and B) carry vapor to and return condensate from each panel. Alternate tubes in each panel are connected to one set of manifold tubes. A diagram of the flow distribution to each panel in each ORU is shown in Figure 9. The manifold tubes at each end of the radiator panels are enclosed by manifold cover plates made of 6061-T6 aluminum and are 5.28" (13.4 cm) wide. The overall length of the panels including the manifold covers is 131.46" (333.9 cm). In order to provide support for the face sheets and increase the strength of the panels, the space between face sheets is filled with a layer of hexcel honeycomb material with a density of 3.1 lb/ft^3 (49.6 kg/m^3). The honeycomb is made of 5052 aluminum foil 0.0007" (0.018 mm) thick.

A moderate temperature (MT) ammonia loop (62° F, 16.6° C) flows through all port side radiator tubes. Two low temperature (LT) ammonia loops (35° F, 1.66° C) flow through alternating tubes in the starboard side radiators. No mass transfer occurs between the two LT ammonia loops, but they may communicate thermally by conduction through the face sheet.

The size of the plumbing of SSF has been optimized to minimize the weight while maintaining the pressure drop in lines at an acceptable level. Therefore, different size tubes are used in the LT and MT loops. Table 1 shows a summary of the plumbing sizes used in this study. The 3 ORU's at each side are pre-integrated on a section of the SSF truss in a folded position for easy transportation and can be deployed on orbit. This requires that the radiator panels in each ORU be connected by flexible tubing that can tolerate folding and unfolding. The manifold tubes of each panel in each ORU are connected to the

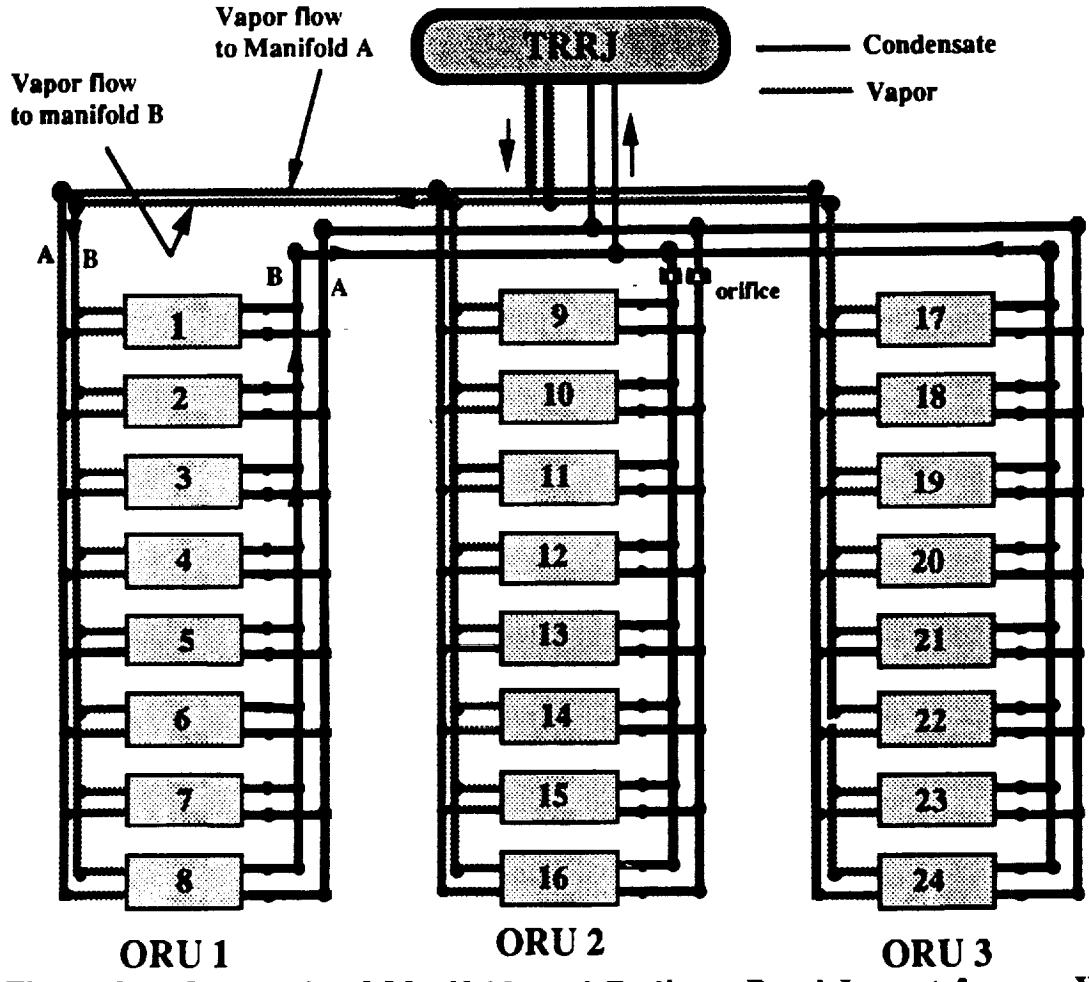

Figure 9 : Schematic of Manifolds and Radiator Panel Layout for one Wing

Table 1: Plumbing Size Summary

	35° F PORT or STBD		62° F	
	ID [inch]	Length [ft]	ID [inch]	Length [ft]
MAIN TRUSS				
liquid	0.466	66.0	0.586	72.0
2-phase	0.952	66.0	1.20	72.0
PACK TRUSS				
liquid	0.466	72.0	0.585	116.0
2-phase	0.706	72.0	0.952	116.0
UMBILICAL				
liquid	0.346	20.0	0.346	20.0
2-phase	0.586	20.0	0.586	20.0
CONDENSER LOOP				
cond. to RFMD	0.466	50.0	0.466	50.0
vapor to panels	0.952	50.0	0.952	50.0
CONDENSERS				
manifold tube	0.939	8.0	0.939	8.0
flex hose	0.805	2.0	0.805	2.0
panel flow tube	0.067	10.07	0.067	10.07

manifold tubes of the next panel in line by flex hose assemblies as shown in Figure 10. The flex hose assembly consists of two pieces of flex hoses and a 180° bend tube section. The loss factor of the flex hoses is estimated as 1.4/ft.

Description of the Detailed Radiator Models

The models described here were developed for detail analysis of the heat rejection system of the ETCS. A simplified representation of the other ETCS subsystems was made in order to maintain size of the models and save computer processing time. The models were developed on version 2.4 of SINDA/FLUINT (ref. 1). Several models with various levels of detail were developed for each configuration of SSF, for MT and LT radiators. However, this study is focused on the analyses performed on the LT radiator models.

Several assumptions were made in developing the models used in the analysis of LT loop radiators. The assumptions were made based on available information at the time the analyses were conducted and the attempt was made to justify validity of these assumptions by comparing the results of the analysis with available data. The water/ammonia interface heat exchangers (IHX) and coldplates (CP) were modeled as point heat sources. The flow rate to each evaporator was calculated by the model such that at the maximum heat load the evaporator vapor quality was 0.8 for the heat exchangers and 0.9 for the coldplates. The estimated pressure drop associated with each IHX or CP was modeled by a LOSS element in line with that IHX or CP.

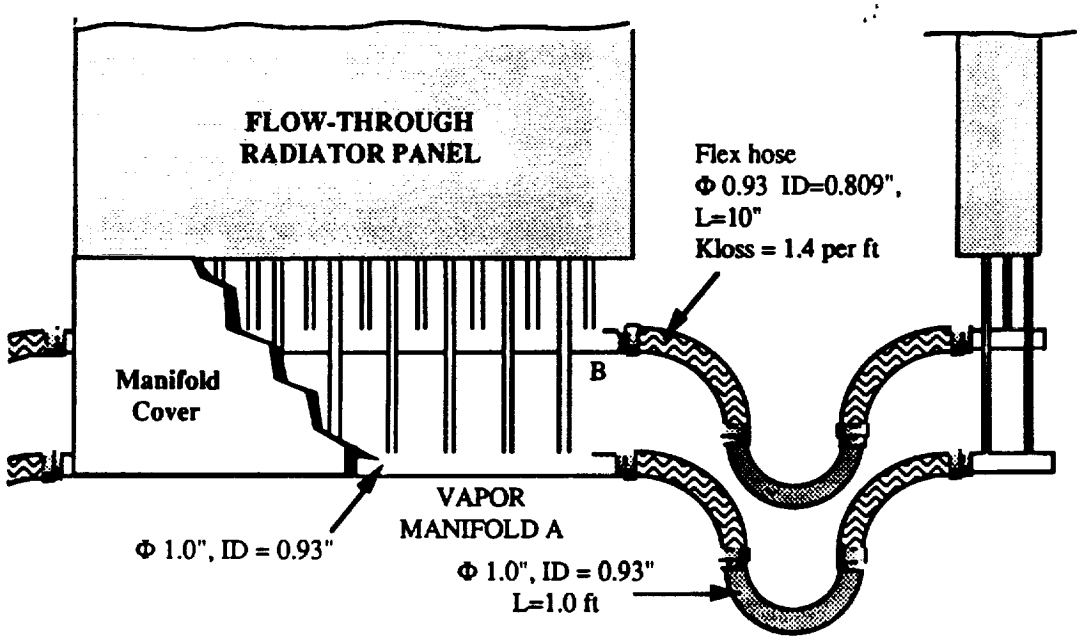

Figure 10 : Arrangement of the Manifold Tubes and Flex Hoses

The rotary fluid management device (RFMD) was modeled by two plena - one representing the warm end set at saturation pressure corresponding to the desired set point temperature, and the other representing the cold end set at subcooled condition. A pressure difference equal to the RFMD end-to-end pressure difference (as reported by the manufacturer) was imposed on two plena. A saturated liquid flow rate equal to the evaporator flow rate plus the RFMD bearing flow and the back pressure regulating valve (BPRV) servo flow was extracted from the warm end plenum. The vapor flow rate out of the RFMD was calculated dynamically by performing an energy and flow balance on the RFMD. The vapor flow rate is a function of the instantaneous heat load, set point of the RFMD, evaporator and condenser return flow conditions, and bearing and servo flow rates. The vapor flow mixes with the BPRV servo flow before entering the radiator panels. The servo flow rate was assumed to vary linearly with total heat load on the system from 0.022 GPM at maximum heat load to 0.015 GPM at minimum heat load (3.35 kW). The BPRV is designed to maintain the RFMD warm end pressure at the set point saturation pressure by regulating the vapor flow rate. The BPRV opening (which determines BPRV pressure drop) is then adjusted to allow sufficient vapor flow out of the RFMD. The model of the BPRV performs the same functions for the normal operations of the system. The BPRV pressure drop in the model varies with vapor flow rate in order to balance the RFMD end-to-end pressure drop. The model will signal if the BPRV reaches its maximum opening and can no longer control the set point.

Several versions of the radiator model with different levels of detail were developed for different analyses. The alternating flow tubes in each radiator panel connect either to LT loop A or B. The flow tubes and other lines and components corresponding to each loop were represented in a separate submodel since no flow mixing occurs between the two loops. Each panel was then represented by models of one flow tube from loop A and one from loop B which were thermally connected through conduction in the face sheet nodes. Each flow tube was modeled by a HX macro with 10 segments in the direction of the flow. The ammonia in each section was represented by a JUNC and the flow tube section was represented by a TUBE with each lump downstream of each tube section.

Condensation Heat Transfer Correlation

The condensation heat transfer coefficient in FLUINT is based on Rohsenow's correlation (ref. 2). This correlation was developed for condensation in annular flows and uses the Martinelli parameter in calculating the two-phase Reynold's number. Transition to single-phase liquid occurs at qualities less than 0.10 and accommodates the breakdown of annular flow into slug flow, using scaling parameters similar to Shah's correlation (ref. 3).

Pressure Drop Correlation

Generally speaking, no single pressure drop correlation can produce accurate predictions of pressure drop for all fluids and flow conditions. The prediction of pressure drop for micro gravity conditions is even more difficult due to uncertainty about the exact flow regime. FLUINT offers a homogeneous (default) and several two-phase pressure drop correlations by setting the IPDC (pressure drop correlation selector) from 0 to 6. Based on the available information at the time of this study, the Lockhart-Martinelli correlation (IPDC=2) was found to best approximate the available data and was used in the models.

Manifold tubes and flex hoses

The schematic of the manifold tubes and flex hoses model for one panel is shown in Figure 11. The loss coefficient and length of the flex hoses that connect the manifold tubes of the adjacent radiator panels were given in Figure 10. A loss coefficient of 4.5 was used for for the flex hose assembly which was modeled by a LOSS connector. Additional LOSS connectors were used to model the pressure drop at the vapor manifold-to-flow tube tee and flow tube-to-condensate manifold tee.

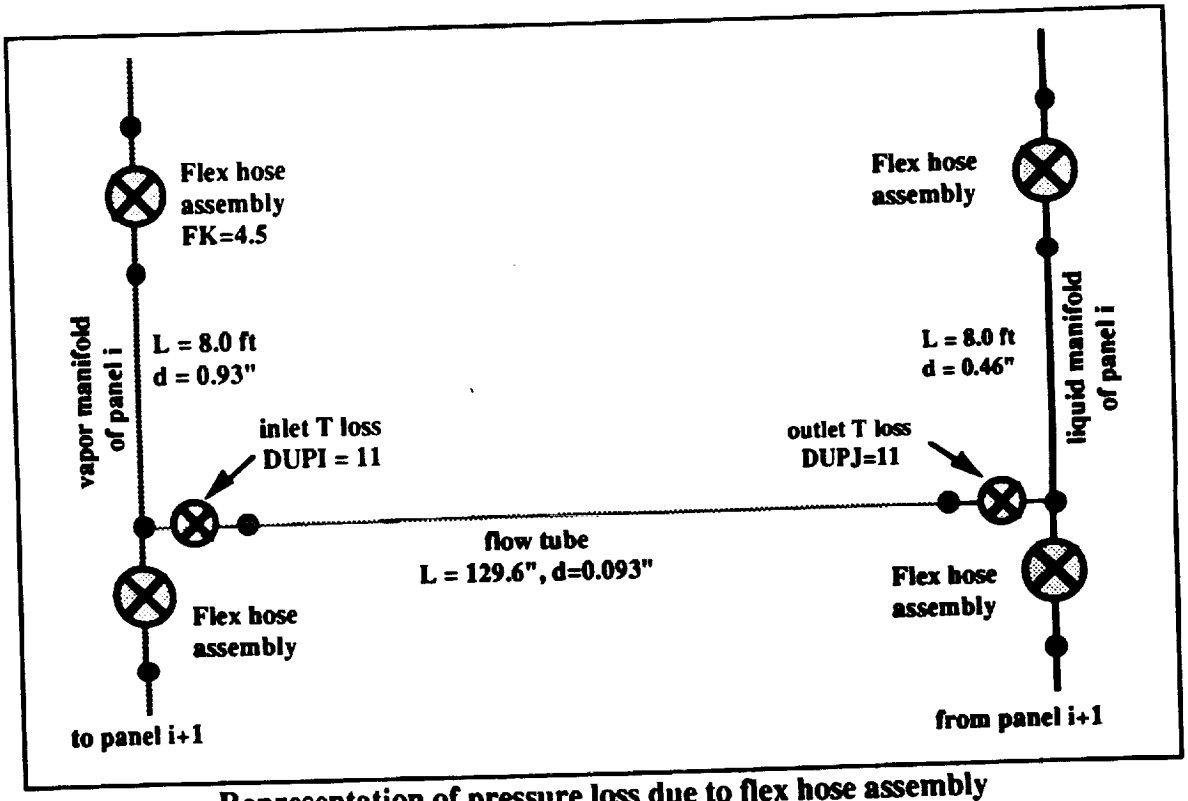

Representation of pressure loss due to flex hose assembly and T's in flow-through panel model

Figure 11: Manifold and Flex Hose Model

Thermal Network

The radiator panel face sheets and extrusion tubes were divided into 10 strips along the panel length. The face sheet area corresponding to each tube segment was 4.73" (12.0 cm) wide, 12.09" (30.7 cm) long, and centered above the tube. The distance of 4.73" (12.0 cm) on the face sheet between the two adjacent tubes modeled was divided into 9 nodes. This nodal break down allowed for determination of the temperature profile of the face sheet between two tubes and eliminated the need for a pre-determined fin efficiency for the radiator face sheet. The nodal breakdown of the radiator face sheet is shown in Figure 12. The mass of each tube segment was represented in the capacitance of the tube wall nodes which was thermally tied to the fluid lump in that tube segment via a heat transfer tie. The flow tube inner wall node was connected to the extrusion inner surface via conductance through the stainless-steel and tube adhesive. The overall conductance of the extrusion tube, from its inner surface to its interface surface, was calculated from a separate detail SINDA model of the extrusion tube. The extrusion interface node was connected to the face sheet node via conduction through the adhesive. The extrusion tube nodes were also connected axially to allow for axial conduction in the subcooled part of the tube. The face sheet nodes were connected both laterally and axially. The thermal network of one segment of two adjacent tubes is shown in Figure 13.

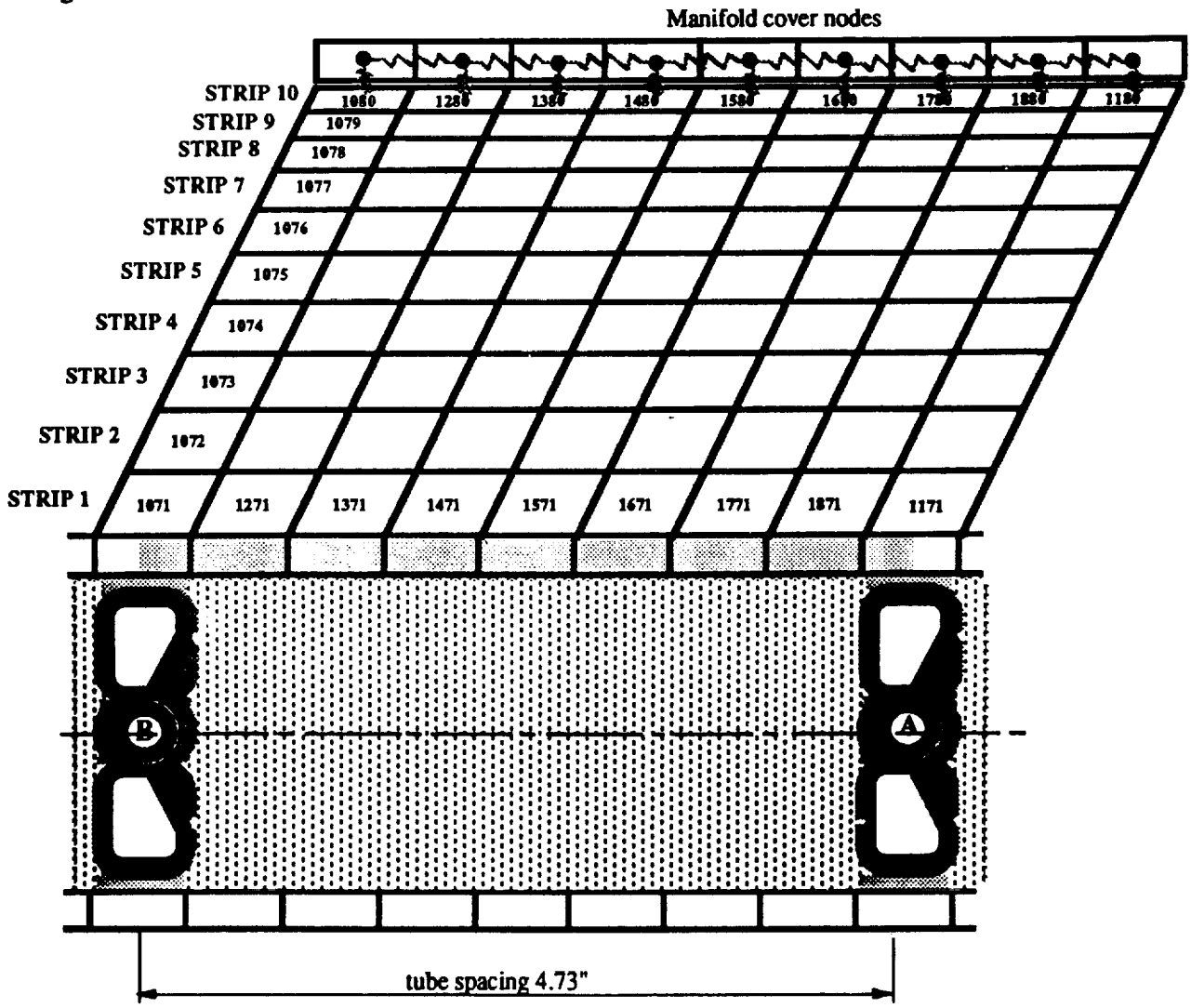

Figure 12: Nodal Breakdown of Radiator Facesheet

The model of the radiator panels was built by using the above described techniques and using a series of DUP's. The DUP option in FLUINT allows the user to simulate the presence of several identical paths without actually modeling them. Each flow tube was DUPed 11 times to represent the 11 tubes per loop in each panel. Each panel was then DUPed 8 times to represent one radiator ORU, and the ORU was in turn DUPed 3 times for representation of the entire radiator array. Another model of the radiator system was developed in which all 22 tubes in one panel were actually modeled. This model was used to study flow variations among the tubes in each panel. A model was also developed in which each panel was represented by two adjacent tubes DUPed 11 times, but all 24 panels were actually modeled. This model was used for study of flow variations among radiator panels due to frictional pressure drop, effects of different environments on each radiator, and effects of isolating some panels or ORU's.

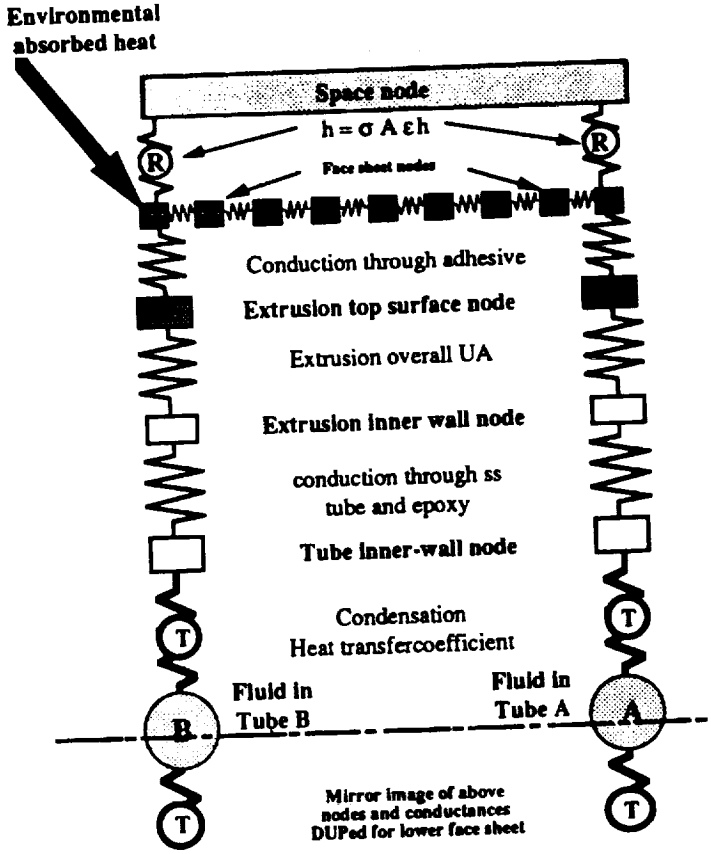

Figure 13: Nodal Breakdown of Radiator Flow Tubes

Counter-flow Radiator Model

The baseline design of the ETCS radiators (described above) consists of two separate loops that flow in alternating tubes of the radiators in the same direction. As a means of increasing the freeze tolerance of the radiators, an alternative arrangement called counter-flow was considered in which the flow in every other tube was in the opposite direction. The arrangement of the manifolds for the parallel (baseline) and the counter-flow option are shown in Figure 14. In the counter-flow option, conduction between loops through the face sheet is very important since the cold end (outlet) of each flow tube is heated by the warm two-phase end of the adjacent tube(s). Results from this study will be presented in addition to the results for the baseline design.

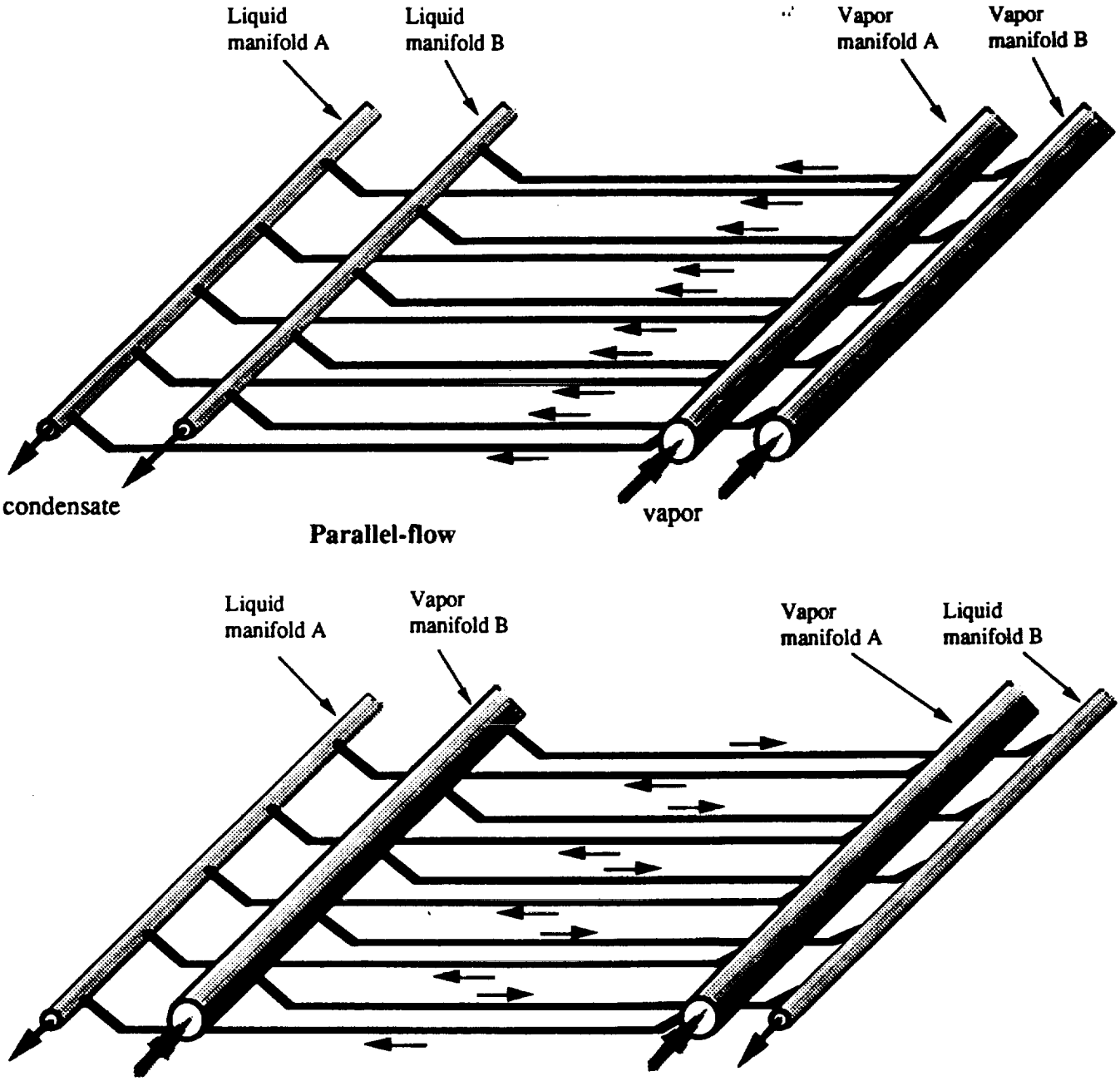

Figure 14: Schematic of the Radiator Panel Manifolds for Parallel and Counterflow

Detailed Radiator Model Analysis Results

The models were analyzed at steady-state and transient conditions for a variety of cases as described below. The Space Station configuration analyzed was the Man Tended Capability (MTC) stage with only one of the radiator ORUs deployed.

MTC Configuration, Warm Case

The MTC configuration model was analyzed at 15 kW heat load and an equivalent effective sink temperature of -50°F (-45.5°C). The heat load was equally split between loops A and B. The results for the two loops were identical and are shown in Table 2. The results indicated that 2-phase ammonia with a vapor quality of 0.967 at 29.3°F (-1.5°C) enters the radiators and exits as subcooled liquid at -32.7°F (-35.9°C). 72.6% of the length of each flow tube was condensing and the rest was subcooling the flow. The panel overall fin efficiency under these conditions was 0.762. The panel overall fin efficiency is the ratio of panel actual heat rejection to ideal heat rejection if the temperature of all the face sheet nodes were equal to the temperature of the hottest face sheet node.

Table 2 : Results of the MTC LT loop analysis at -50° F sink temperature

	Flow Rate Lb/hr	Heat Load [KW]	Inlet Temp [F]	Inlet quality	Outlet Temp [F]	Condensing Fraction
Loop A	0.498	7.5	29.37	0.967	-32.7	0.726
Loop B	0.498	7.5	29.37	0.967	-32.9	0.726

MTC Configuration, Cold Case

An effective sink temperatures of -95°F (-70.5°C) was used to represent a typical radiator cold environment (no freezing). The results of the MTC configuration analysis for a 15 kW total heat load are shown in Table 3. The results indicated that the ammonia outlet temperature was subcooled at -83.9°F (-64.4°C).

The model was run for the same cold case conditions as above with a radiator counter-flow configuration to examine the effectiveness of the counterflow design in raising the radiator outlet temperature. The results shown in Table 3 indicated that the radiator outlet temperature was 84.5°F (47°C) warmer for the counter-flow case. The ammonia temperature profiles in each flow tube for the parallel and counter-flow cases are shown in Figure 15. The results indicated that although condensation was completed faster in the counter-flow case, the subcooling of the condensate flow at the outlet was much less due to heat leak from the 2-phase ammonia in the adjacent tube. The coldest ammonia temperature in the counter-flow case was -60°F (-51.1°C) and occurred in the middle of the panel. The panel overall fin efficiencies for the parallel and counter-flow cases were 0.54 and 0.55, respectively.

Table 3 : Results of the MTC LT loop analysis at -95° F sink temperature

	Flow Rate Lb/hr	Heat Load [KW]	Inlet Temp [F]	Inlet quality	Outlet Temp [F]	Condensing Fraction
Parallel flow	0.457	7.5	29.1	0.97	-83.9	0.48
Counter-flow	0.528	7.5	29.1	0.97	0.6	0.29

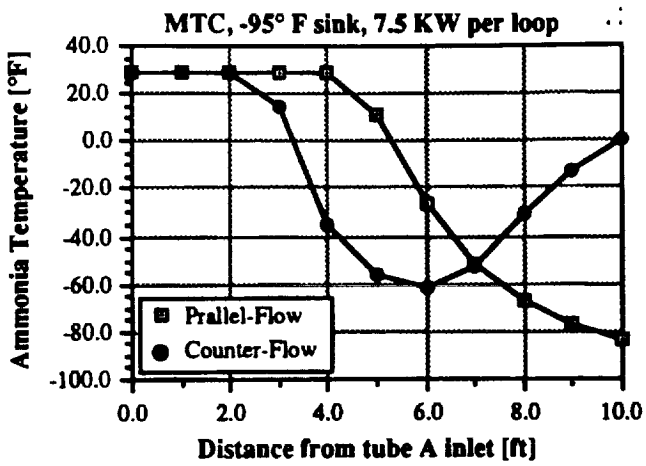

Figure 15: Ammonia Temperature Profile in Flow Tube A for Parallel and Counterflow

Radiator Freeze Prevention Studies

Under low heat loads and very cold environments when the effective sink temperature falls below the freezing temperature of ammonia (-108°F, -78°C), the fluid in the radiators may freeze. This leads to very high local pressures inside the flow tubes when frozen ammonia begin to thaw. During the SSF ETCS design process, the problem of radiator freezing (and subsequent thawing) was addressed. One approach was to try to increase the radiator condensate return temperature in cold cases without limiting its heat rejection capability in hot cases. Other approaches allowed the ammonia to freeze and thaw under controlled conditions. Several of the options which were investigated using the detailed SINDA/FLUINT radiator models are presented here.

Freeze Prevention by Radiator Pointing

The MTC configuration of SSF was analyzed with two heat loads at transient conditions using a cold case environment (orbit angle Beta=0°, beginning of life surface properties) and different radiator orientations. The results are shown in Table 4. The coldest environment was the "edge-to-sun on the sun side"/"edge-to-earth on the dark side" (ETS/ETE) orientation, which resulted in radiator freezing for some

Table 4 : Summary of the results of MTC configuration transient analysis under cold environment at β=0, for different radiator panels orientation

PANEL ORIENTATION sunside/darkside	N0. of Panels	Condensate return temp. [° F]	
		4.0 kw	11.2 kw
ETS/ETE	8	freezing	freezing
ETS/FTE	8	-106	-95 to -100
FTE/FTE	8	-29 to -51	-
45°-to-earth	8	-62 to -75	-33 to -81

parts of the orbit for both heat loads. The "face-to-earth on the sun side"/"face-to-earth on the dark side" (FTE/FTE) orientation was the warmest environment, but resulted in a reduced heat rejection capacity of the radiators on the sun side of the orbit. The results indicated that the situation was improved and freezing was prevented as panel orientation was changed to face the earth on the dark side of each orbit. However, the large pitch angle in the SSF torque equilibrium attitude (TEA) significantly limited the possibility of radiator pointing to modifying the radiator environment, and resulted in environments that were much colder. Therefore, this option alone was not sufficient to prevent radiator freezing.

Freeze Prevention by Increasing BPRV Liquid Flow or Heating Radiators

Using the SINDA/FLUINT models, a study was conducted to examine the feasibility of other options such as increasing the BPRV liquid servo flow or electrically heating radiator flow tubes in order to prevent radiator freezing (ref. 4). The 4-orbit cold case design sink temperature profile for Beta=0° and TEA=0°, shown in Figure 16, was used in the study. The results of the study showed that increasing BPRV servo flow had no significant effects on radiator outlet temperature. The change in radiator outlet temperature was negligible even when BPRV servo flow rate was increased by 20 times its normal value. Next, the model was analyzed at 3.35 kW heat load with simulated electrical heaters bonded to the extrusion tubes. The heaters were turned on only during the dark side of each orbit. The results indicated that 5.28 kW of electrical power was required in order to maintain radiator outlet temperatures above -90°F (-67.8°C). Use of that much power would have an unacceptable impact on SSF.

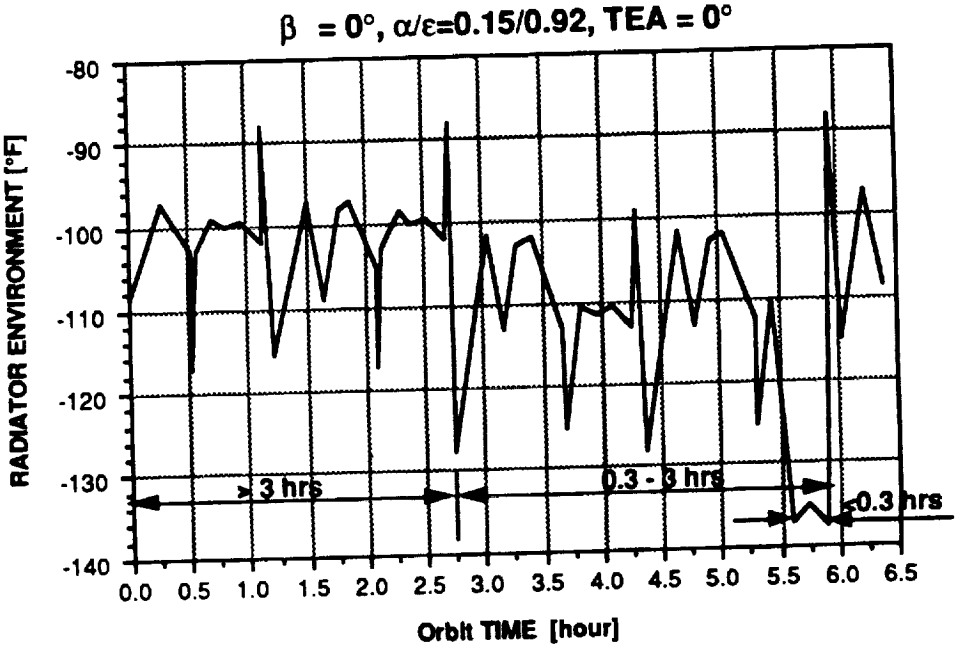

Figure 16: Cold Case Sink Temperature Profile for Coldest Panel

Freeze Prevention with Counter-flow Radiators

The counter-flow radiator design (described above) was another option that was considered since it does not increase the weight of the radiators and does not require any additional components. This option eventually gave way to a SSF design solution in which some of the condensate tubes were allowed to freeze and thaw without bursting. For the SSF case, the freeze/thaw design solution was used since it works even when one of the low temperature loops is not flowing; however, in other applications the counter-flow option may be the best design solution to deal with radiator freezing.

A case was run using the MTC model at low loads (3.35 kW per loop), using the coldest panel environment for Beta=0 and TEA=-45° as shown in Figure 17. The results of the analysis using the parallel-flow (baseline) option are shown in Figure 18. The results showed that freezing of ammonia occurred at sub-freezing sink temperature parts of the orbit. The results of the analysis with the counter-flow model are shown in Figure 19. Unlike the parallel flow case, the coldest fluid temperature in the counter-flow design occurs at the middle of the radiator panels since the condensate return flow at the outlet of each tube is warmed up by the 2-phase flow at the inlet of the adjacent tubes. Figure 19 shows the radiator condensate return temperature as well as the radiator coldest fluid temperature and indicates that the freezing problem was eliminated by the counter-flow option.

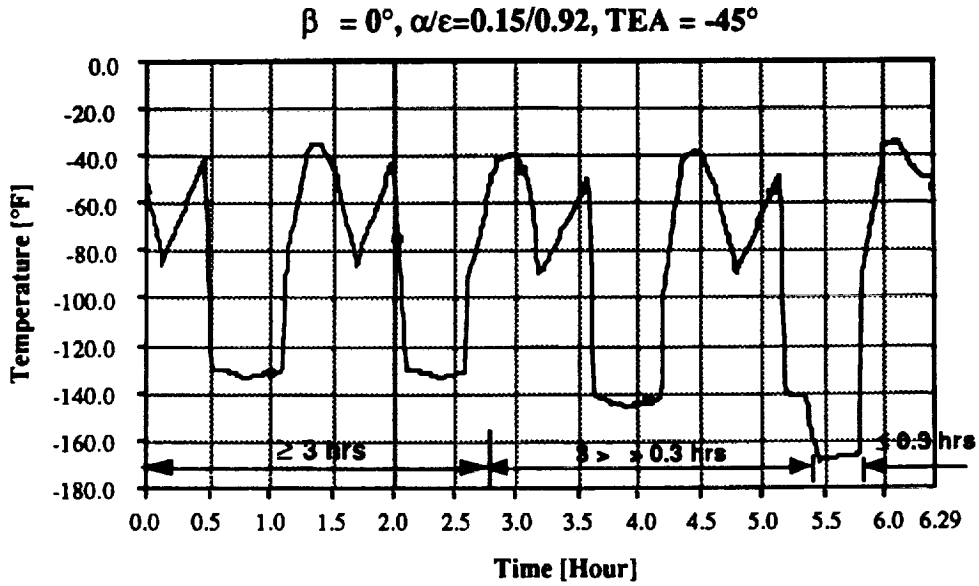

Figure 17: Coldest panel environment for MB5 configuration

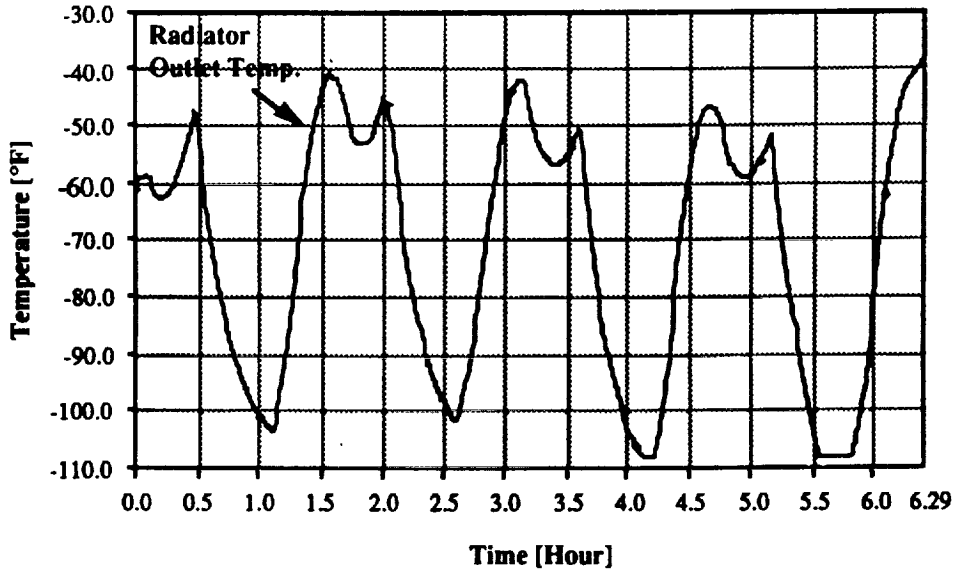

Figure 18: Parallel-flow Radiator Exit Temp. (Beta=0°, TEA=-45°, 3.35 kW per loop)

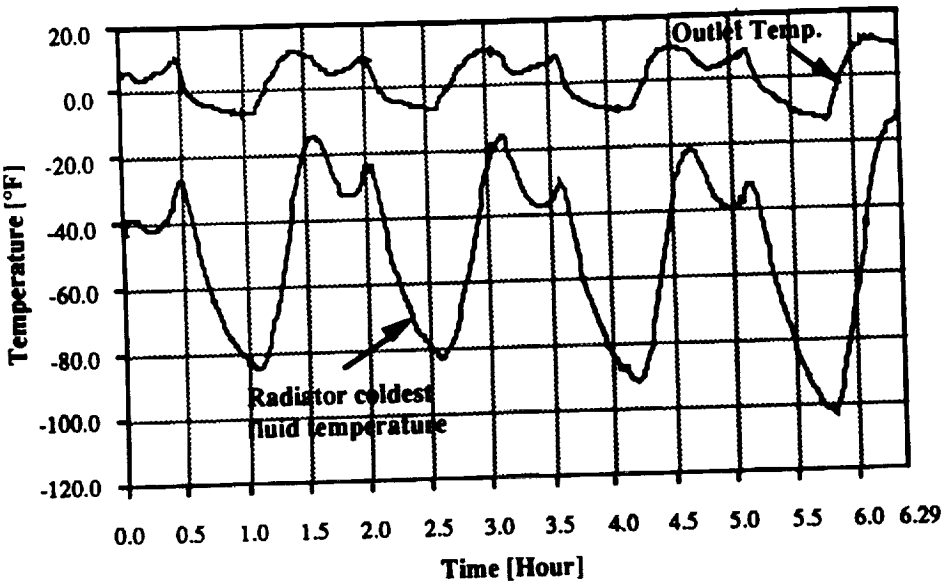

Figure 19: Counterflow Radiator Temperatures (Beta=0°, TEA=-45°, 3.35 kW per loop)

Detailed Radiator Models Summary

SINDA/FLUINT is a powerful tool for detailed analysis of complicated thermal and fluid systems. The detailed models developed at JSC for the analysis of the Space Station ETCS radiators have been essential in predicting performance of the radiators for many nominal and off-nominal conditions of practical interest. The models have been used to study such design problems as response to orbital environment transients and radiator freezing.

IDEAL GAS SYSTEMS

The Space Shuttle's ATCS, the SSF Internal Thermal Control System, and the flow of propellant are all aerospace systems involving single-phase liquid flow. In addition to these applications, the filling and evacuation of rigid containers by a gas is another situation where single-phase flows are encountered.

From thermodynamics, when a gas is compressed or expanded isentropically and adiabatically, its temperature will increase or decrease, as described by the integrated, isentropic forms of the Gibb's equation (decompression) or the first law of thermodynamics (compression) modified by the ideal gas law [eqn. 1]. However, if this gas is contained in a non-adiabatic tank, heat transfer with the side walls will affect the thermal response of the gas and the simple equations relating pressure and temperature will be complicated. In general, the introduction of heat transfer terms into these governing equations prevents a closed-form solution and a numerical model must be developed. The SINDA/FLUINT program can be used to solve these problems.

The Basic SINDA/FLUINT Model

Figure 20 presents the schematic of a basic SINDA/FLUINT model that can be used the predict pressurization and depressurization of gaseous system. The gas storage container is represented by the TANK option which allows calculation of transient pressure and temperature changes as mass is removed from or added to the system. To account for possible environmental heat losses, the TANK is tied thermally to a SINDA model (or an individual node) of the storage container by the use of a convection

heat transfer (HTU) tie. The value of this tie must be determined for each specific application. System flow rates are controlled by the MFRSET (Mass Flow Rate SET). The plenum (PLEN) is used to represent an infinite source of supply gas or a reservoir to dump the exhaust gas. The TANK is connected to the PLEN by an STUBE (Short TUBE) which can, if User Logic is employed, represent a pressure drop device (such as a regulator or an orifice). The working fluid is modeled as an ideal gas by using 8000 series fluid data blocks.

To ensure that this model was properly developed, the predicted final temperatures were compared against the theoretical results for adiabatic filling and isentropic, emptying processes for dry air. For a tank emptying process with constant thermophysical properties, the equation for the final temperature is (ref. 5),

$$T_f = \frac{T_i}{\left(\frac{P_i}{P_f}\right)^{\frac{k-1}{k}}} \qquad [1]$$

where T_f is the final temperature, T_i is the initial temperature, P_f is the final pressure, P_i is the initial pressure and k is the ratio of the specific heats.

For a filling process, the following equation may be used (ref. 6),

$$T_f = \frac{kP_fT_{in}T_i}{(P_f - P_i)T_i + kP_iT_{in}} \qquad [2]$$

where T_{in} is the temperature of the inlet gas.

For the range of parameters to be considered here, the predicted results from the SINDA/FLUINT model were within 0.5 °F (0.3 K)of the theoretical results of both equations. The slight discrepancy is due to use of constant properties (k) in the theoretical equations, while the numerical model employs variable properties. From this comparison study, it was felt that the model was properly developed for filling and evacuation processes.

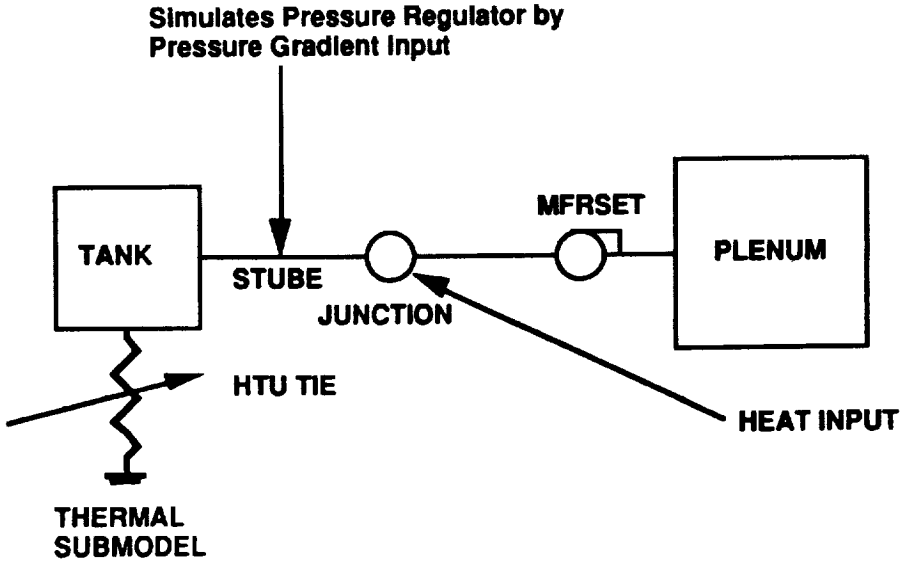

Figure 20: Schematic of the Gaseous System SINDA/FLUINT Model

Space Station Freedom Airlock

During the life of the Space Station Freedom (SSF), the crews will be required to perform a variety of Extra-Vehicular Activities (EVAs), in order to maintain the station. Before entering the vacuum of space, the EVA teams will perform a variety of breathing exercises to condition themselves for the EVA. Once these breathing exercises are completed, the crew enters the airlock, evacuates the chamber by using a vacuum pump and journeys outside.

If during the EVA (or some other time) a crew member is exposed to a low pressure environment, it is possible that he will experience decompression sickness (the bends). To avoid returning to Earth and to provide quick medical treatment, the SSF airlock will be used as a hyperbaric treatment facility. To perform this medical treatment process, the airlock is pressurized to 2.8 atmospheres and the affected crew member(s) undergo a variety of breathing exercises. To reduce the high temperatures associated with compression, a heat exchanger is included as part of the airlock hardware.

As evident from equations [1] and [2], the gases within the airlock will exhibit substantial changes in temperature. In addition to fluid temperature variations due to pressure changes, heat transfer to the side walls and heat removal by the heat exchanger will also affect system response. To understand how these phenomena interact and affect the airlock gas temperature and pressure, a detailed model including all the aforementioned effects was developed.

Development of the Numerical Model

Figure 21 shows a schematic of the airlock which is depicted as a right circular cylinder, 6.22 ft (2.00 meters) in diameter and 8.22 ft (2.50 meters) in length. Located on one wall of the airlock is a fan and cross-flow heat exchanger assembly which is used to cool the chamber during hyperbaric operations. Also included in this package is a centrifugal vacuum pump which is used to depressurize the chamber for EVAs.

Before a numerical model of this system could be developed, certain simplifying assumptions for both the air and specific mechanical aspects of the airlock were made. These assumptions are listed below.

1) The gases within the airlock may be considered ideal. For the conditions examined here, the compressibility factor (Z in most thermodynamics textbooks (ref. 6)) is nearly unity, indicating ideal gas conditions. As a result, the thermophysical properties of gas considered varies only with temperature.
2) At any given time, the gas within the chamber is at a uniform temperature. That is, there are no temperature gradients across the airlock gas.
3) Since the flow inside the airlock during the withdrawal process is low velocity and laminar, convection effects will be ignored. On the other hand, during hyperbaric operations the fan is on and produces substantial flow velocities. To account for this convection, the heat transfer coefficient will be the same as that of the Space Shuttle.
4) Due to the lack of gravity, there are no natural convection effects.
5) The gas is dry so heat transfer effects due to condensation are ignored.
6) The gas within the airlock is not a participating media.
7) The airlock is constructed out of 6061 aluminum and at a uniform temperature.
8) The heat exchanger is modeled using the NTU method (ref. 7).
9) There are no heat losses to the environment.

Figure 22 shows a schematic of the SINDA/FLUINT airlock model, which is the same as the model shown in Figure 20 with several minor modifications. The gas is represented with the TANK option and is tied to a single thermal diffusion (time-dependent) node which represents the airlock's metal mass so that convective heat transfer effects can be included. The PLEN represents either the hyperbaric

charging tanks or the vacuum of space. The MFRSET has been replaced by a VFRSET (Volume Flow Rate SET) to provide a more accurate representation of the vacuum pump.

The hyperbaric heat exchanger is modeled with its own loop, and more specifically with a pair of junctions. To determine its heat removal rate, the following approach was taken. First, the NTU method (ref. 7,8) was applied using the characteristics of a preliminary heat exchanger design (ref. 9) and its outlet air temperature was determined. With the outlet thermodynamic state determined, the CHGLMP (CHanGe LuMP) option was used to alter the current state to the new and more accurate condition and the HTRLMP (HeaTeR LuMP) option was used to hold the current state. The HTRLMP option maintains the desired thermodynamic state by supplying an appropriate heat load at the downstream junction.

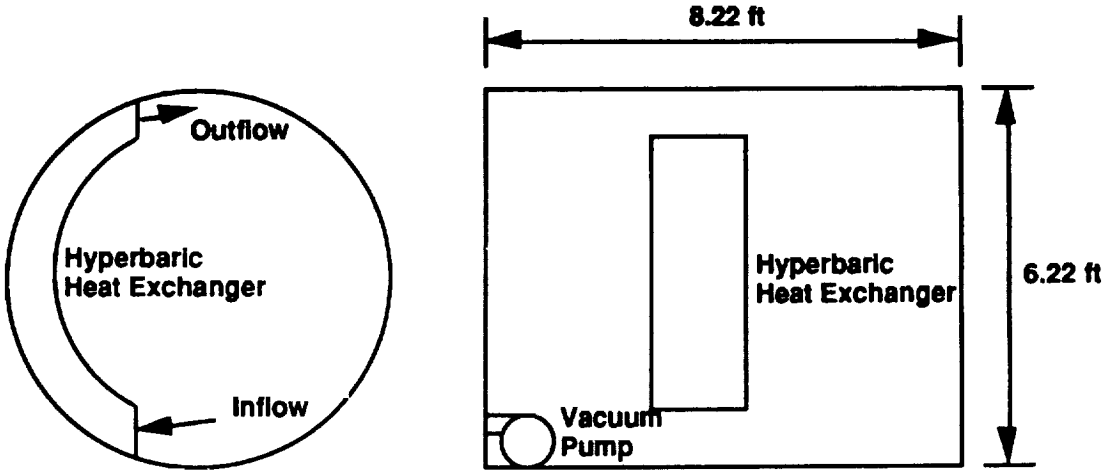

Figure 21: Schematic of SSF Airlock.

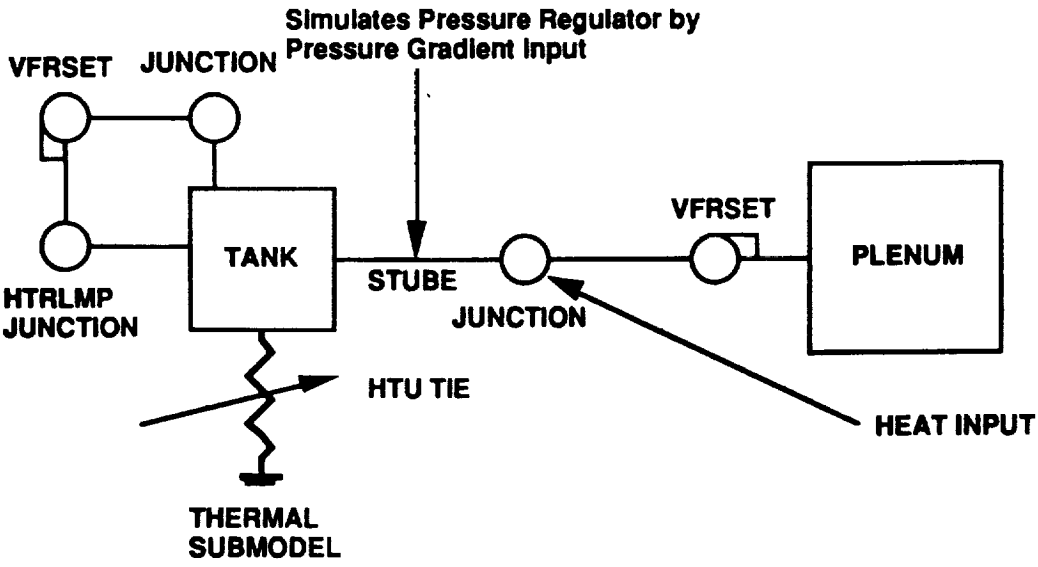

Figure 22: Schematic of the SINDA/FLUINT Airlock Model.

Depressurization Results

The model was first used to predict the thermal response of the airlock gas as it is depressurized from 10.2 psia (70.3 kPa) to 0.5 psia (3.4 kPa). For this situation, three depressurization times were considered: 5.0, 7.5 and 10.0 minutes. Since the hyperbaric heat exchanger does not operate during this phase of airlock operations, the HTRLMP option was taken out of the model. In addition, since convection is miniscule, the value of the heat transfer tie was set to zero.

Figure 23 shows the predicted thermal response of the airlock gas for the three cases with an inlet charge air temperature of 70 °F (294.3 K). Since there is no heat transfer for any of these cases, they all reach the same minimum temperature of -235 °F (125 K). While these low temperatures may be encountered, it should be noted that the crew members will be suited and should remain unaffected.

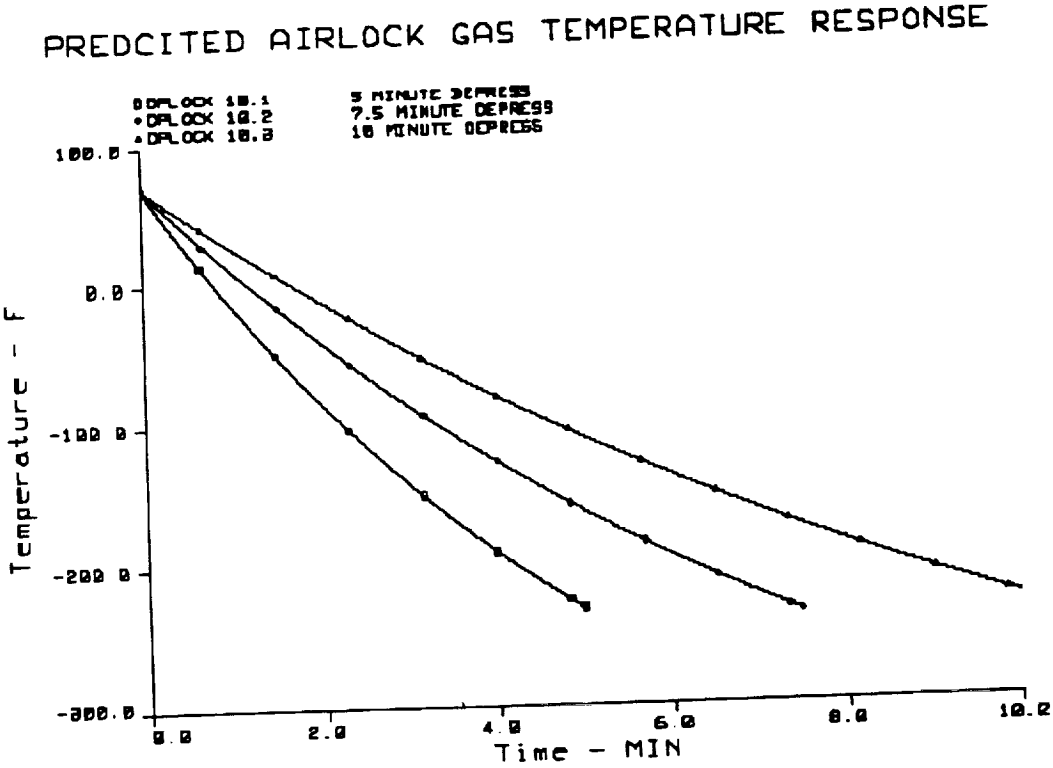

Figure 23: Predicted Airlock Depressurization Gas Temperature Response

Hyperbaric Results

The model was next used to determine the thermal response of the airlock gas during hyperbaric pressurization to 2.8 atmospheres for three different cases with a pressurization rate of 13.2 psi/min (91.0 kPa/min), 70 °F (294.3 K) charge air and an equipment heat load of 1440 Watts. The first case considered an adiabatic situation. The second case included convection with the side walls. Finally, the last case considered the combined effect of the heat exchanger and convective heat transfer.

Figure 24 shows the predicted temperature response of the airlock gas for the three test cases examined. These results show that heat transfer effects can substantially reduce gas temperatures. Specifically, when convection is include the maximum temperature is reduced by approximately 50 °F (28 K) while the operation of the heat exchanger reduces the maximum temperature another 50 °F (28 K) to a comfortable range.

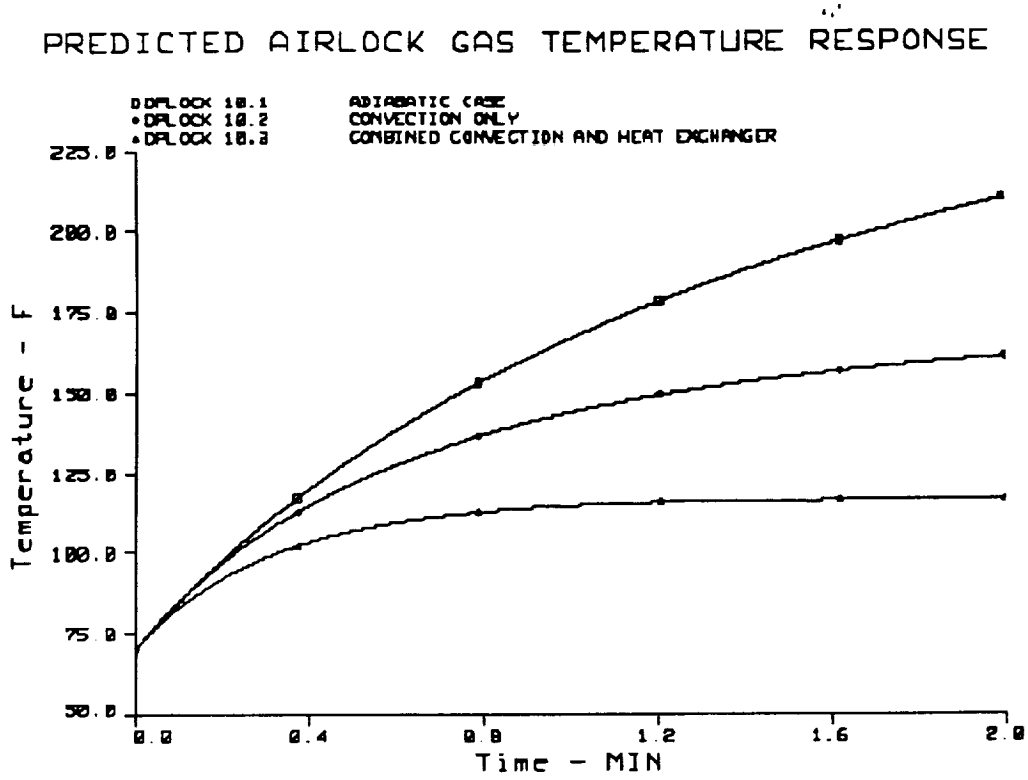

Figure 24: Predicted Temperature Response for Three Different Heat Transfer Cases

During normal operations, the charge air tanks will be heated and cooled by radiative heat transfer with the environment. It is estimated that due to this heat transfer, the temperature of the charge air may vary from 70 °F (294.3 K) to 0 °F (255.4 K). As indicated by equation [2], for a filling process, the final temperature is influenced by the incoming gas temperature, so it follows that charge air temperature will be important during hyperbaric operations. To examine the effect of charge air temperature on system response, four inlet air temperature were used: 10 °F (261 K), 30 °F (272.1 K), 50 °F (283 K), and 70 °F (294.3 K). The charge air was used to pressurize the chamber to 2.8 atm at 13.2 psi/min while the heat exchanger was operating.

Figure 25 presents the thermal response of the airlock gas during pressurization for the four charge air temperatures. From these results it is clear that the temperature of the incoming air plays an important role in chamber temperature response.

Airlock Model Summary and Conclusions

From this study, it was found that convective heat transfer is important in determining airlock gas temperature. By using the heat exchanger , the severity of the high temperatures associated with the compression processes will be lessened. Finally, depress temperatures are low but should be no problem for suited astronauts.

The Simplified Aid for EVA Rescue Device

During the construction phase of the Space Station, astronauts will be required to perform many long-duration EVAs. While conducting these EVAs, it is possible that an astronaut may become separated

from the SSF tethers and float free. Since the Space Shuttle cannot maneuver safely in this construction environment and retrieve the wayward astronaut, an alternative rescue approach must be employed.

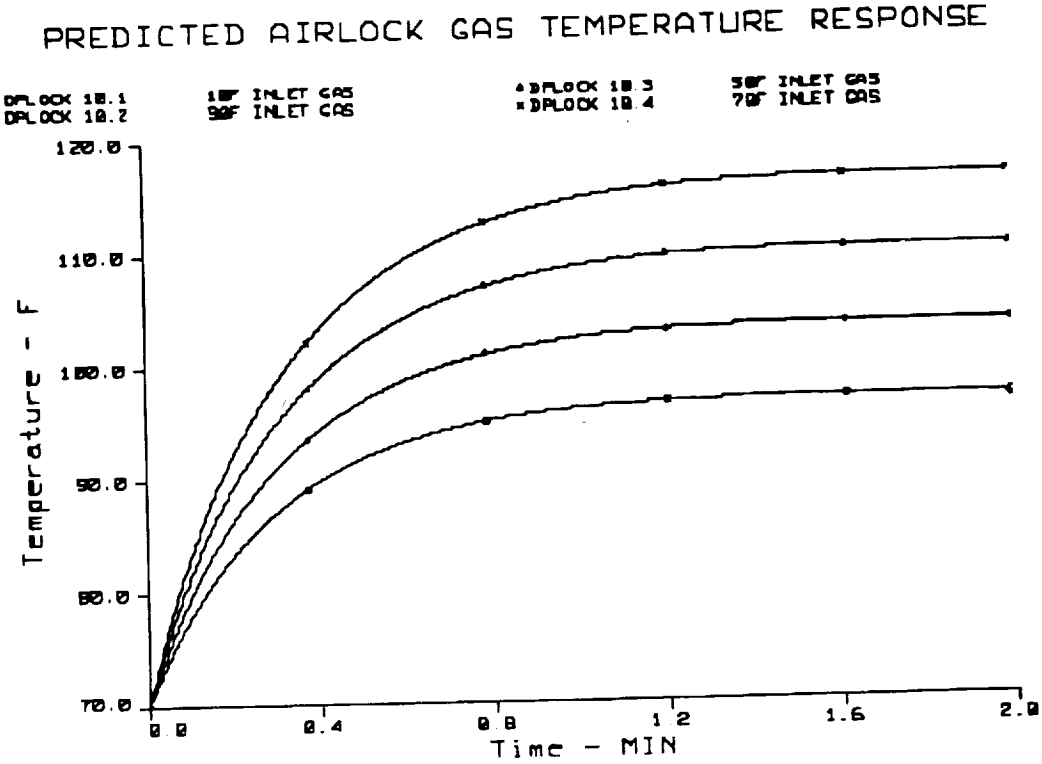

Figure 25: Predicted Response for Four Different Inlet Gas Temperatures

One possible rescue method employs the Simplified Aid For EVA Rescue (SAFER) system. Here, before the EVA begins, a small thruster back pack is attached to the rear of the astronaut's space suit, and then worn throughout the duration of the space walk. This back pack consists of four main propulsion thrusters and 12 smaller course correction nozzles, all of which are fed high pressure, non-reacting gas from a storage tank. Currently, the supply gas is xenon, since it requires the smallest containment vessel compared to other candidate gases. Due to its high molecular weight, gas leakage is minimal (ref. 10). If, during the EVA, an emergency arises, the SAFER system is activated, the astronaut fires the thrusters and guides himself to a place of safety.

As can be shown by the governing equations for supersonic nozzle flow (ref. 11), the performance of the SAFER thrusters depends almost exclusively on the thermodynamic state and properties of the working fluid at the inlet of the propulsion nozzles which is supplied from the storage tank. Since mass is removed from the storage tank during SAFER operation, expansion effects will cause the state within the storage tank to change, ultimately affecting the inlet conditions to the nozzles. In addition, the gas storage bottle radiates to deep space and cools (it may lose heat for six to ten hours before the the thrusters are fired), creating lower tank pressures and temperatures which affect nozzle performance when the thrusters are required. As a result (and as will be shown), the choice of fluid and thermal response of the storage tank have a significant impact on the performance, size and weight of the SAFER system.

Development of the Numerical Models

The SAFER system presents several unique heat transfer and thermodynamic situations which do not lend themselves to simple closed-form solutions. First, the transient cooling of the storage tank by

radiative heat transfer to deep space is described by a non-linear differential equation, and except for a few idealized cases cannot be solved. The SAFER system cannot be treated as an idealized thermal radiator, since it also exhibits conduction and re-radiation, complicating the problem and making an analytical solution impossible. Second, the propulsion thrusters are supersonic nozzles and their performance is determined by nozzle inlet and storage tank conditions, but the storage tank pressure and temperature are dependent upon the mass flow rate out of the thrusters. It is clear then from the above examples, that both situations are quite complex and numerical models must be developed.

Storage Tank Model

The first situation to be examined was the radiative cooling of the storage tank gas before the thrusters are fired, since these results are important in the development and analysis of the thruster model. This model considers the heat loss of the gas and gas containment system to deep space during the EVA, before any propellant is used.

Figure 26 presents a simple schematic of the propellant tank. Here, the xenon gas is contained in a rigid metal pressure vessel, which is protected from meteoroid impacts by a thin metal shield. The entire apparatus is then placed in a holding mount within the plastic (maybe fiberglass) SAFER shell and surrounded with Multi-Layer Insulation (MLI). The gaps between the spheres may be evacuated or filled with MLI. The dimensions listed on this figure are only preliminary (ref. 11) since many factors (choice of nozzle, amount of line heating, amount of gas), which have yet to be accurately determined, influence the tank size.

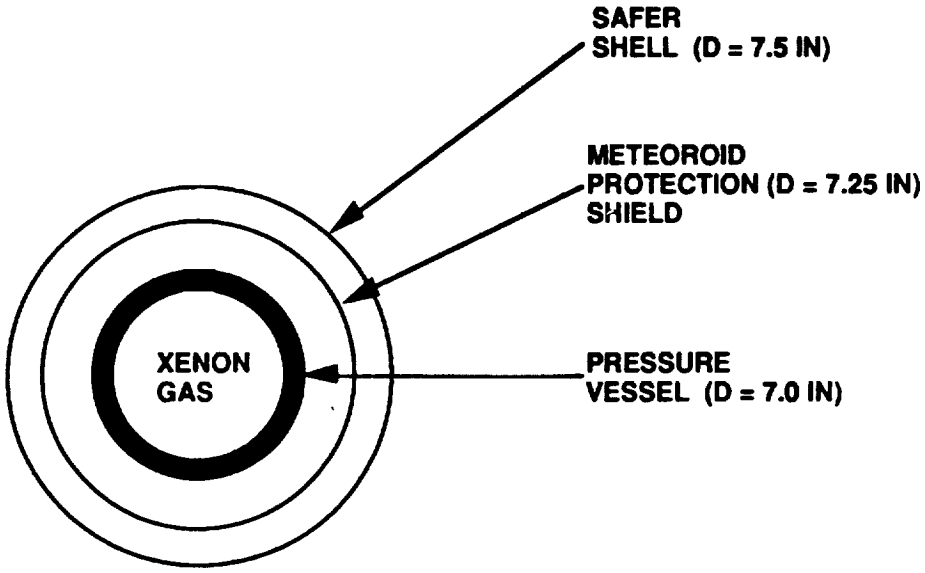

Figure 26: Schematic of the Storage Tank

Before the numerical model was developed, certain simplifying assumptions were made. Assumptions were made for both the gas and its holding vessel and these are listed below.

1) The pressure vessel and meteoroid shield are constructed out of stainless steel.
2) Xenon is the only gas considered. The model will be developed so that other gases can be considered.
3) Preliminary weight estimates are; 16.0 lbm (7.25 kg) for xenon, 10.6 lbm (4.80 kg) for the pressure vessel, and 0.5 lbm (0.23 kg) for the meteoroid shield (ref. 11).
4) The pressure vessel, meteoroid shield and SAFER shell are treated as concentric spheres. The conduction and radiation conductors for this situation are found by the method outlined in reference 9.

5) Only the worst case cooling situation will be considered. That is, there is no incident radiation from the Sun, SSF, Space Shuttle or Earth on any portion of the SAFER system.
6) MLI is used as the insulating material.
7) When appropriate, there is no conduction between spheres.
8) No fluid is withdrawn from the tank, since this model examines the quiescent fluid before thruster firing.
9) Radiating surfaces have an effective emissivity of 0.05.

The development of a SINDA/FLUINT model for the storage tank is a relatively simple task. First, each piece of the storage tank assembly is considered a model node and its thermal capacitance is determined (mass multiplied by specific heat). Next, the heat transfer conductors between the each node are determined by using the methods outlined in References 1 and 7. With this accomplished, a boundary condition (node) is set for deep space at - 460 °F (-273.2 K) and the FWDBCK method (ref. 1) is used to determine the transient cooling process.

Storage Tank Model Results

In order to understand what factors influence the radiative cooling of the storage tank and to suggest appropriate control methods, several test cases must be examined. For the present study, five cases were examined. Four of the five cases considered radiation as the sole means of heat transport to the deep space environment. That is, the heat transfer between the containment spheres occurs only by thermal radiation. Using Figure 26 as a guide, the four radiation cases considered are: xenon only (Case 1), xenon and the pressure vessel (Case 2), xenon, the pressure vessel and the meteoroid shield (Case 3), xenon, the pressure vessel, the meteoroid shield and the SAFER shell (Case 4). Case 5 considers the same conditions as Case 4 except the evacuated spaces between the spheres is filled with MLI (12 layers) which has an effective emissivity, ε^*, of 0.05. For all cases, heat is eventually rejected to the cold environment of space by radiation, over a maximum period of 16 hours.

Figure 27 presents the transient thermal response of the storage tank gas for the five insulating cases as they radiate heat to space over a period of 16 hours. These results are also summarized in Table 5. As can be seen, Case 1 (xenon only) exhibits substantial and unacceptable cooling; however, with the inclusion of the pressure vessel (the minimum design requirement), the temperature drop is severely reduced, since there is additional mass which must cooled. The use of the meteoroid shield substantially reduces the heat loss, since it acts as a thermal radiation shield (heat transfer barrier). Similarly, the inclusion of the SAFER holding shell further reduces the heat losses. When the entire system is considered, with the MLI included, the heat leak is minimal (4 °F (2.2K) after 16 hours), indicating that a passive scheme can provide acceptable results and eliminate the need for a heater on the pressure vessel.

The Storage Tank/Thruster Model

Figure 28 presents a simple schematic of the thruster system. Here, gas from the storage tank flows into a pressure regulator to ensure that a constant pressure is maintained at the nozzle inlet over the entire time of thruster operation. The working fluid then flows from the regulator outlet to the thruster nozzles where it is expanded isentropically in a supersonic nozzle to provide thrust for the back pack. Since a thruster design (manufacturer) has yet to be chosen, the exact working pressures, temperatures, nozzle areas and flow rates of this system are not known.

Before the thruster model was developed, the following simplifying assumptions were made:
1) All the candidate gases (argon, xenon, nitrogen) are considered ideal, even at the storage tank condition of 8000 psia. At the nozzle inlet (after the regulator) the pressures are low enough (approximately 500 - 1000 psia) that the gases behave ideally and the relationships for ideal supersonic flow may be used. The appropriate governing equations will be presented shortly.
2) The regulator performs as an ideal throttling device (enthalpy is constant), thus for ideal gases there is no temperature drop.

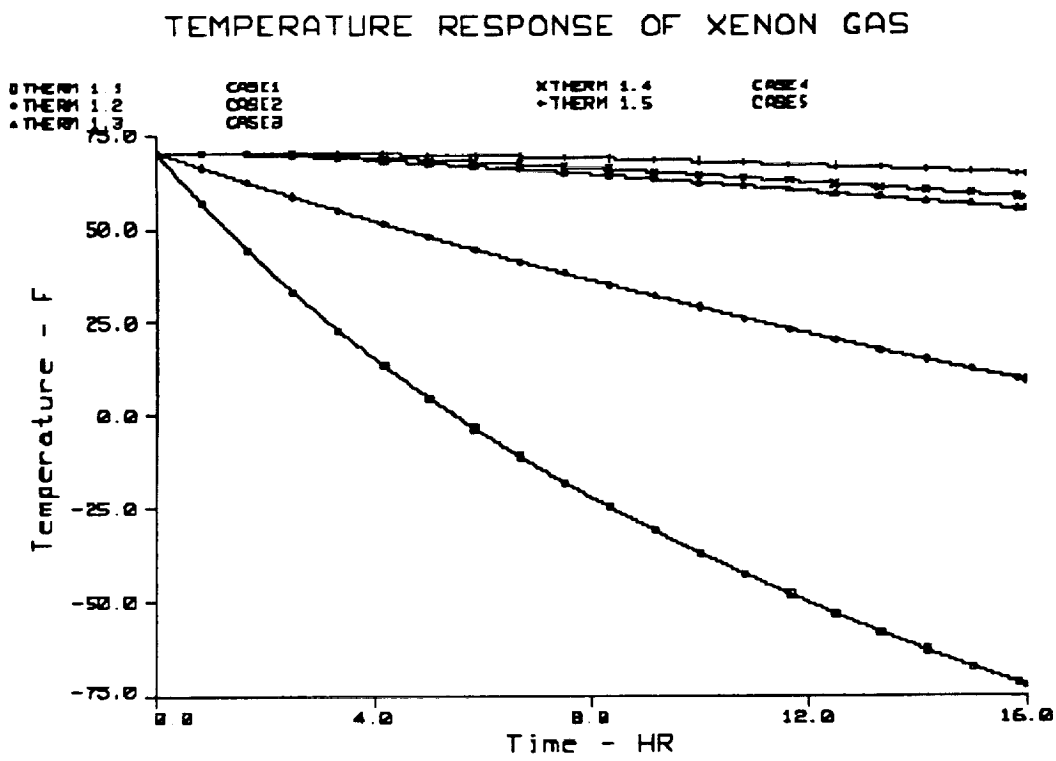

Figure 27: Predicted Cooling of Storage Tank by Radiation for Five Insulating Cases

Table 5: Predicted Gas Storage Temperatures at Various Times for Different Insulating Conditions with the Initial Temperature Set at 70 °F and the Deep Space Environment Set at -460 °F.

Insulating Condition	Temperature After 6 Hours (°F)	Temperature After 10 Hours (°F)
Case 1	0	-25
Case 2	50	40
Case 3	65	60
Case 4	66	64
Case 5	68	67

3) The convection in the storage tank due to mass removal may be modeled as described in reference 12.
4) The thermal model developed to predict environmental heat leak may be incorporated into this model.
5) The thrusters and regulator performance will be based on the most recently available data (ref 11). The model will be built in such a way as to accommodate changes in thruster design.
6) The storage tank volumes of the three gases in cubic feet (meters) are; 0.223 (0.00631), 0.122 (0.00345), 0.307 (0.00869) for argon, xenon and nitrogen, respectively.

Figure 20 was used to model the SAFER system. The storage tank is represented by the TANK option which allows calculation of transient pressure and temperature changes as mass is removed from the tank. To account for the environmental heat loss, the TANK is tied thermally to the previously developed SINDA model of the storage container by the use of a convection heat transfer (HTU) tie. The

value of this tie is determined by the method outlined in reference 12 for determining convection in exhausting spherical pressure vessels. The regulator is represented using the STUBE option and a junction (JUNC). Since the storage tank pressure changes, user logic is employed in the main program to alter the pressure across the STUBE (the HC term) so that the required pressure is maintained at the junction. This junction also represents the inlet to the nozzle and it is here that inlet heating is applied. The nozzle is modeled using an MFRSET where the mass flow of this device is governed by the following equation,

$$m = A_t * P_o * \sqrt{\frac{k * G_c}{T_o * R} * \left(\frac{2}{k+1}\right)^{\left(\frac{k+1}{k-1}\right)}} \qquad [3]$$

where, A_t is the nozzle throat area, P_o is the nozzle inlet pressure, k is the ratio of specific heats, G_c is the conversion factor, R is the specific gas constant, and T_o is the nozzle inlet temperature. Since T_o varies as the storage tank is depressurized the mass flow rate is updated at each iteration. Because A_t and P_o are specific to a given thruster, these quantities are input to equation [3].

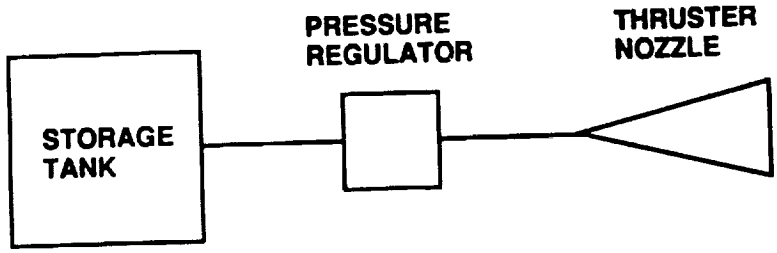

Figure 28: Schematic of the SAFER System.

Results for the Storage Tank/ Thruster Model

For the thruster study, two flow situations were examined. First, the model was run with and without heating of the incoming gas to examine system response. Finally, three candidate gases (argon, xenon, nitrogen) were examined for identical operating conditions to determine their individual effects on the thermal response of the storage tank and system performance. For all cases considered, the initial condition of the storage tank was 8000 psia (55.2 MPa)and 70 °F (294.3 K).

The model was next run to examine the effect of heating the inlet gas on system performance. Figure 29 shows the predicted thruster mass flow rate, with xenon as the working fluid, with and without heating during a one minute operation period. For the heated condition, the nozzle inlet temperature is maintained at the initial conditions of 70 °F (294.3 K), while for the unheated situation, the inlet nozzle temperature is identical to the storage tank temperature. From these results, it is clear that inlet heating is beneficial, since at the end of the run an approximately 30% greater mass flow rate is required to maintain the same performance. In other words, without inlet heating, propellant will be consumed at a faster rate. Of course, this problem could be alleviated by using a larger storage tank; however, the SAFER system would be larger and bulkier.

To further examine what factors influence system performance, the model was next run for three different working fluids for identical operating conditions, including heating of the inlet gas to 70 °F (294.3 K). Figure 30 presents the thermal response of the storage tank for one minute of thruster operation. Here, nitrogen shows a substantially higher tank temperature than the other two gases. Since the thermal response of the gas within the tank is governed by the equation [1], it follows that gases with higher k values will produce lower tank temperatures during depressurization. Since argon and xenon have higher values of k than nitrogen, it follows that their storage tank temperatures must drop more quickly than nitrogen.

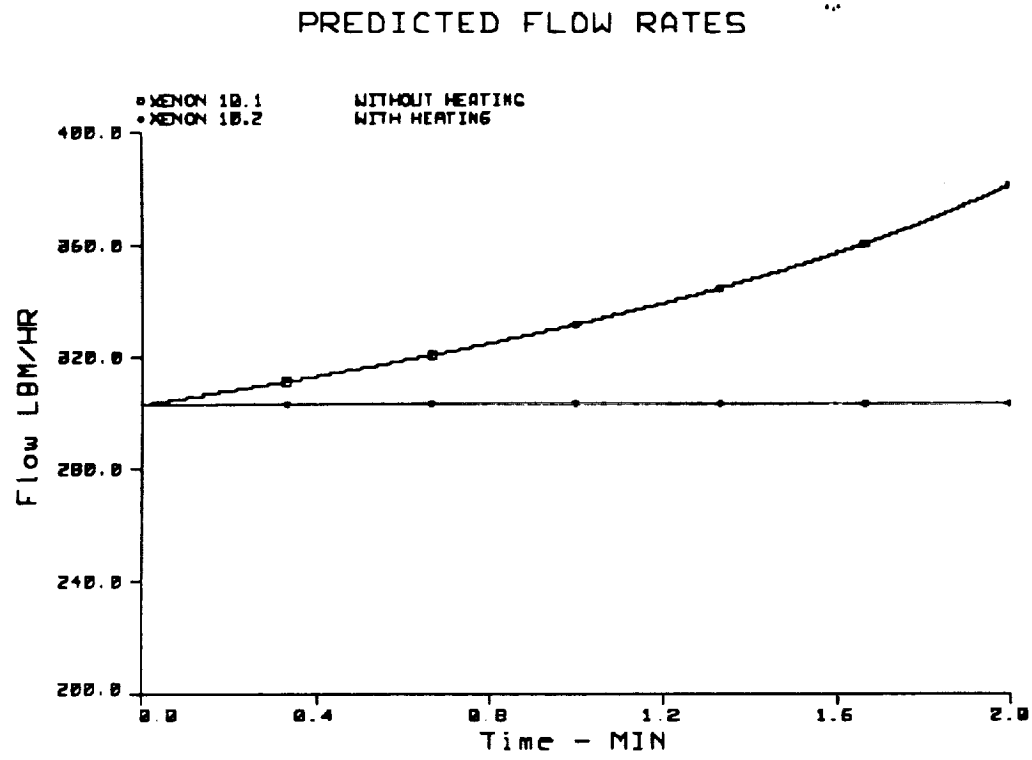

Figure 29: Predicted Mass Flowrates for Heated and Unheated Inlet Gas

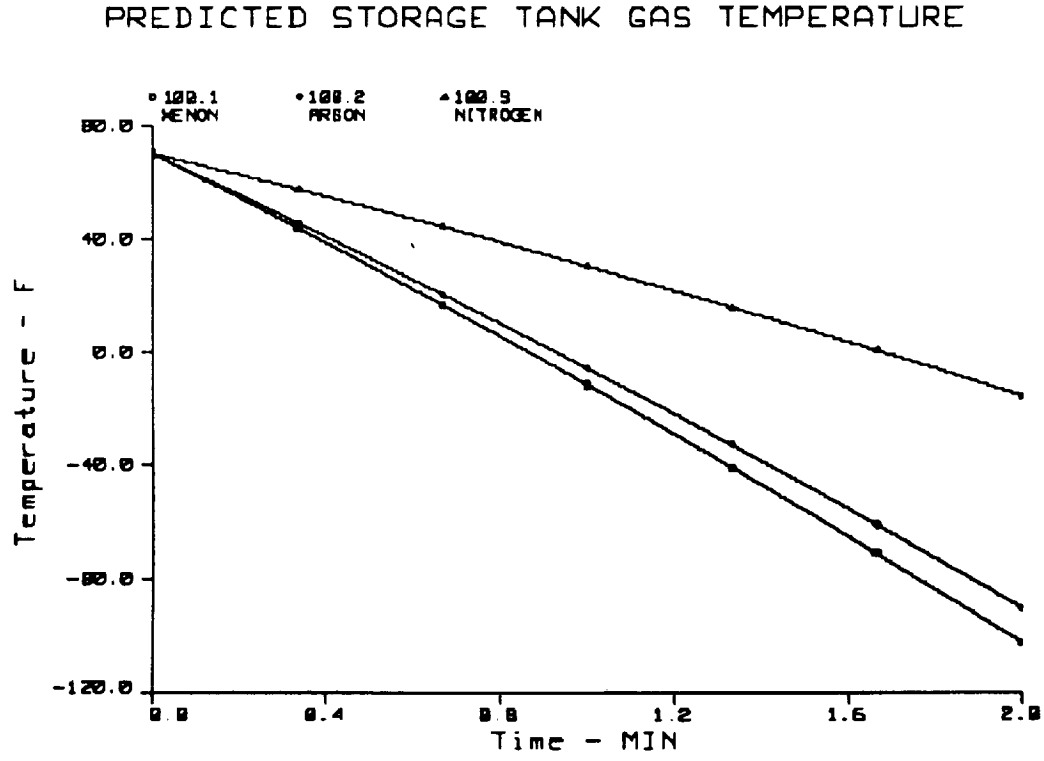

Figure 30: Predicted Thermal Response of the Storage Tank for Three Candidate Gases

While the results of Figure 30 suggest that nitrogen would need the least amount of inlet heating (smallest temperature difference between the initial, 70 °F (294.3 K), and the tank temperature), attention is directed to Figure 31 which shows that over the period of operation, xenon requires the least amount of heating. For this situation, the heating of the gas can be determined from the first law of thermodynamics ($Q = mC_p(70\text{-}T_{Tank})$) and of the three candidate gases, xenon has the lowest specific heat. As a result, from a heating point of view, it recommended that xenon be used as the working fluid, since it requires the least amount of heating.

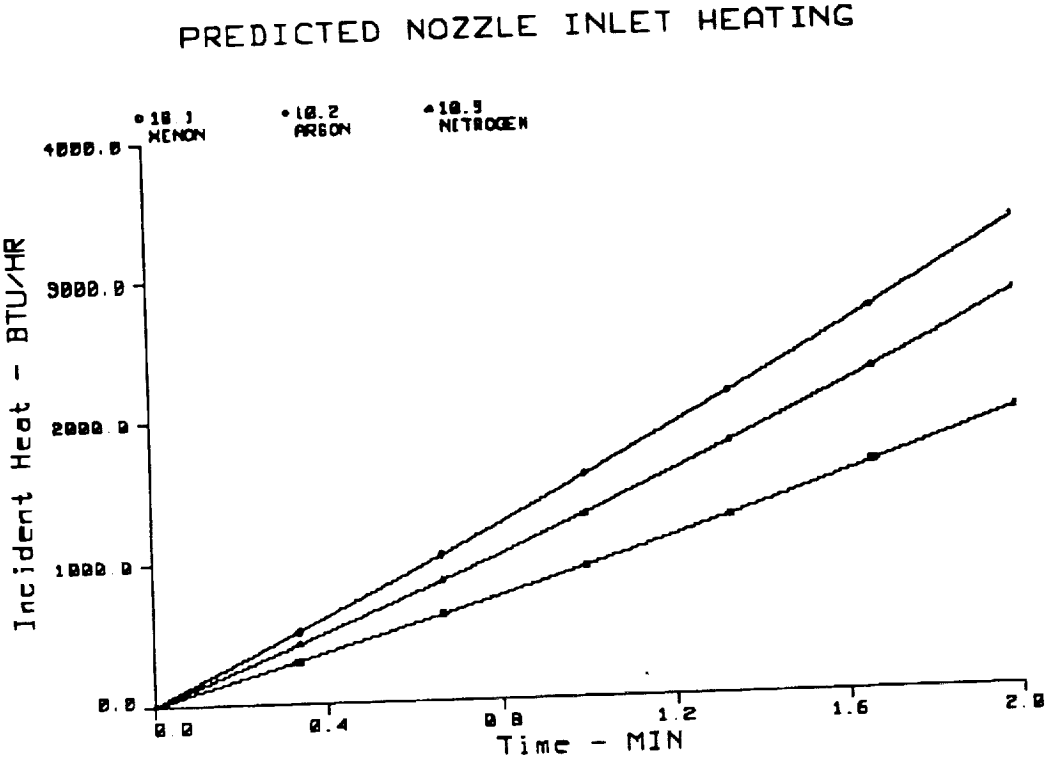

Figure 31: Predicted Heat Addition to Maintain the Inlet at 70°F for Three Gases

SAFER Summary and Conclusions

Two SINDA/FLUINT models have been developed to predict the transient thermal and hydrodynamic response of various components of the SAFER system and serve as a design tool. Since the exact thruster design has yet to be chosen, the models have been built so that they can be easily modified to handle any changes in working fluid, thruster design, insulating materials and pressure regulators.

One model predicts the thermal response of the storage tank as it radiates to space. This model predicts that with a simple MLI insulating scheme and a meteoroid shield, there will be minimal heat leak to the environment during the EVA time (sixteen hours or less).

The other model predicts the thermodynamic performance of the thrusters and the thermal response of the storage tank during thruster operation. The results indicate that heating of the inlet gas is beneficial, by reducing thruster mass flow rates, in turn reducing the size of the tank. In addition, preliminary results indicate that xenon should be chosen as the propellant, since it requires the lowest heat input to maintain the required conditions.

CONCLUSION

Because of its versatility, SINDA/FLUINT has been applied to a wide variety of aerospace problems at JSC and elsewhere. For different problems, different features of the code have been used. Some aspects of the code which have been utilized at JSC include transient simulation, boiling and condensation, two-phase flow pressure drop, slip flow, multiple submodels and depressurization. Several of these applications have been described in this paper. Use of SINDA/FLUINT by the aerospace community and others continues to increase as the capabilities of the code expand (ref. 13).

REFERENCES

1. Cullimore, B., et al., SINDA/FLUINT Systems Improved Numerical Differencing Analyzer and Fluid Integrator, Version 2.4, User's Manual, December 1991.

2. Rohsenow and Harnett, Handbook of Heat Transfer, 1973.

3. Shah, M. M., 'A General Correlation for Heat Transfer During Film Condensation Inside Pipes', Int. Journal of Heat & Mass Transfer, Vol. 22, pp 547-556, 1979.

4. DeMarchi, D., 'Freeze Prevention of Ammonia in the CTB Radiators', Lockheed Engineering and Sciences Co. Technical Memorandum, LESC-30053, Jan. 1992.

5. VanWylen, G.J., and Sonntag, R.E., Fundamentals of Classical Thermodynamics, 3rd ed., John Wiley and Sons, New York, 1986.

6. Loomis, A.W., Compressed Air and Gas Data, Ingersoll-Rand, New Jersey, 1980.

7. Incropera, F.P., and DeWitt, D.P., Fundamentals of Heat and Mass Transfer, John Wiley and Sons, New York, 1985.

8. Kays, W.M., and London, A.L., Compact Heat Exchangers, 3rd ed., McGraw-Hill, New York, 1984.

9. "Analysis Report - Hyperbaric Chamber Heat Loads and Removal Methods," prepared by Eagle Technical Services Inc., Houston, Tx. for Lockheed Missiles and Space Company, Inc., Houston, Tx.

10. SAFER Pre-Preliminary Design Review, May 1991.

11. Shapiro, A.H., The Dynamics and Thermodynamics of Compressible Fluid Flow, Vol. 1, John Wiley and Sons, New York, 1953.

12. McKinney, P.H., "An Investigation of the Thermodynamic Performance of a Discharging Spherical Pressure Vessel", Ph.D. Thesis, Rice University, 1973.

13. Cullimore, B. A. , Ring, S. G. and Ungar, E. K., "Development Status of SINDA/FLUINT and SINAPS", Fourth Annual Thermal and Fluids Analysis Workshop, NASA Lewis Research Center, August 17-21, 1992.